NASA TN D-238

TECHNICAL NOTE

D- 238

THE DEPENDENCY OF PENETRATION ON THE MOMENTUM PER UNIT AREA OF THE IMPACTING PROJECTILE AND THE RESISTANCE OF MATERIALS TO PENETRATION

By Rufus D. Collins, Jr., and William H. Kinard

Langley Research Center
Langley Field, Va.

NATIONAL AERONAUTICS AND SPACE ADMINISTRATION

WASHINGTON

May 1960

NATIONAL AERONAUTICS AND SPACE ADMINISTRATION

TECHNICAL NOTE D-238

THE DEPENDENCY OF PENETRATION ON THE MOMENTUM PER UNIT AREA OF THE IMPACTING PROJECTILE AND THE RESISTANCE OF MATERIALS TO PENETRATION

By Rufus D. Collins, Jr., and William H. Kinard

SUMMARY

The results of this investigation indicate that the penetration of projectiles into quasi-infinite targets can be correlated as a function of the maximum momentum per unit area possessed by the projectiles. The penetration of projectiles into aluminum, copper, and steel targets was found to be a linear function while the penetration into lead targets was a nonlinear function of the momentum per unit area of the impacting projectiles. Penetration varied inversely as the projectile density and the elastic modulus of the target material for a given projectile momentum per unit area.

Crater volumes were found to be a linear function of the kinetic energy of the projectile, the greater volumes being obtained in the target materials which had the lowest yield strength and the lowest speed of sound.

INTRODUCTION

With the development of rockets capable of propelling vehicles beyond our immediate atmosphere and into the regions of space, the problem of predicting and understanding the damage which may result if the vehicle is impacted by meteorites has become critical. Designers of these vehicles must have some means of determining the skin necessary to defeat the meteorites likely to impact.

The problems of studying impacts of particles traveling at speeds in the meteorite velocity range (reported to be between 30,000 to 240,000 feet per second) are unsurmountable at the present time since no known means exists to accelerate particles having appreciable mass to these velocities in the laboratory. As a result, impact data must be taken in much lower velocity realms with the hope of understanding

the phenomena to expect at higher velocity impacts. The impact data presented herein were obtained in the velocity range below 12,000 feet per second.

A survey of existing penetration equations made prior to the collection of these data lead to the establishing of a possible physical picture and explanation for the penetration phenomena. The data of this investigation were then obtained to substantiate this explanation.

SYMBOLS

a	speed of sound in target material, $\sqrt{E/\rho}$, ft/sec
A	constant of proportionality defined by equation (7)
B	quantity of energy necessary to produce cratering, ft-lb
C	quantity of momentum necessary to produce penetration, lb-sec/sq in.
d	diameter, in.
E	Young's modulus
L	maximum length of projectile normal to point of impact
K	constant of proportionality defined by equation (5)
m	mass of projectile, slugs
P	penetration, in.
V	projectile velocity, ft/sec
v	crater volume, cu in.
ρ	mass density, slugs/cu in.

Subscripts:

p	projectile
t	target
c	crater

APPARATUS AND TEST TECHNIQUE

Description of Projectiles and Targets

Four materials were used in this investigation for the projectiles and targets. The materials were commercially pure copper bar stock, 2024T-3 aluminum bar stock, commercially pure lead, and cold rolled steel having a carbon range from 0.12 to 0.30 and a manganese range from 0.30 to 0.60. This selection of materials provided 16 different projectile-target material combinations with which to study the behavior of high-velocity impacts. These four materials were chosen on the basis of their greatly different density, strength properties, and speed of sound in the materials.

The projectiles fired in this investigation were spheres having diameters of 0.0625 inch, 0.22 inch, and 0.50 inch and cylinders having diameters of 0.22 inch and 0.50 inch with a length-diameter ratio L/d equal to 1.

The targets were all large compared with the crater volumes produced and were in most cases at least five times as thick as the depth of penetration. Target size was chosen in order that the target might be considered as semi-infinite with respect to the projectile.

Accelerators

Photographs of the three guns used to accelerate the cylinders and spheres are shown in figures 1 to 3. Figures 1 and 2 show, respectively, a conventional 0.220-caliber Swift rifle and a 0.50-caliber gun which were used to accelerate the projectiles to velocities in the neighborhood of 6,000 feet per second.

Figure 3 shows the helium gas gun which was used to accelerate projectiles to velocities approaching 13,000 feet per second. The helium gun consists of a 20-millimeter compressor tube and a 0.22-inch-diameter smooth bore launch tube which is connected to a large vacuum chamber. A powder charge was placed in the breech end of the compressor tube and the compressor tube charged with helium to a pressure of 1,000 pounds per square inch. The burning-powder charge provided a shock front which compressed the helium gas and provided the force necessary to launch the projectile at the desired velocity. The launch tube and vacuum chamber were evacuated to a pressure below 1 inch of mercury; thus the aerodynamic drag was reduced and greater projectile velocities could be obtained.

REVIEW OF PENETRATION EQUATIONS

Numerous studies have been conducted by various investigators concerning the phenomena of high velocity impacts. The results have consisted primarily of data which could be defined by empirical equations over some limited range of impact conditions. Among the existing penetration equations is one by Huth, Thompson, and Van Valkenburg which is established in reference 1. This equation relates penetration as a function of the ratio of impact velocity to the speed of sound in the target material. The ratio V/a is commonly referred to as the impact Mach number and is related to the target penetration by the equation

L
7
6
6

$$P = dK\left(\frac{V}{a}\right)^{1.4} \tag{1}$$

which covers the range $0.1 < \frac{V}{a} < 1.0$ when target and projectile are of the same material.

Charters and Locke in reference 2 reported that the penetration of spheres in lead and copper targets could be correlated as a function of the impact Mach number and the ratio of the projectile density to the target density ρ_p/ρ_t. The results of their investigation indicated that the equation

$$\frac{P}{d} = 2.28\left(\frac{\rho_p}{\rho_t}\right)^{0.69}\left(\frac{V}{a}\right)^{0.69} \tag{2}$$

described the line faired through their data points.

The investigation conducted in reference 3 to determine the effect of target temperature also utilized the product of the density ratio ρ_p/ρ_t and the impact Mach number V/a. The data obtained in this test program appeared to be described by the equation

$$\frac{P}{d} = K\,\frac{V}{a}\,\frac{\rho_p}{\rho_t} \tag{3}$$

where the value of K depended upon the shape of the projectile and the target material.

A study of the parameters in these equations was made to determine a physical explanation of the impact cratering. It was noted in the equations listed that the projectile density, velocity, and length (or

diameter) were of significant importance in predicting target penetration. An analysis of these three terms revealed that their product is actually the momentum per unit area possessed by a projectile. The product of the projectile mass density and the velocity is the momentum per unit volume of the projectile. This value when multiplied by the maximum projectile length will yield the maximum momentum per unit frontal area possessed by the projectile as shown in figure 4. Physically, the projectile can be pictured as a bundle of rods with axes in the line of projectile travel and having a unit cross section, the length of each rod being equal to the length of the projectile at their corresponding location.

The cratering effects of a projectile into a target can be pictured as the impact resulting from the collisions of individual rods. The maximum penetration will then occur at the point on the target surface impacted by the longest rod, whose length is equal to the maximum length of the projectile along the axis of travel.

From this analysis it appears that target penetration should be expressed by the relationship

$$P = f\left(\rho_p VL\right) \tag{4}$$

Actually, it is realized that there are forces between the imaginary rods during the projectile impact and that each rod does not maintain its original shape but deforms. Therefore, a factor must be included in the penetration equation to account for the projectile deformation. This factor should be proportional to the physical properties of the projectile. A factor must also be included to represent the resistance to penetration offered by a target.

PRESENTATION OF RESULTS

The penetration data obtained during this investigation has been presented in table I and illustrated graphically in figures 5 to 8. Data (from ref. 4) are included in figure 8 for a 3/16-inch sphere. The penetration achieved by the projectiles was correlated as a function of the maximum momentum per unit area of the projectile. Figures 9 and 10 show, respectively, the dependence of penetration on the density of the projectile and the elastic modulus of the target material.

The ratio of crater diameter to projectile diameter has been shown graphically in figures 11 to 14 as a function of the projectile velocity.

In figures 15 to 18 the crater volumes have been plotted as a function of the effective kinetic energy of the projectile for the 16 different projectile-target combinations.

DISCUSSION

Penetration Equations

The penetration data obtained in this test program with the exception of impacts into lead targets were defined by the equation

$$P = K(\rho_p VL - C) \tag{5}$$

and are shown graphically in figures 5 to 7. The value of C in equation (5) was simply the intercept of the curve on the axis of momentum per unit area. The fact that all curves did not pass through the origin was expected because of the elastic properties of the materials. In order to produce permanent penetration, enough momentum must be available in the $\rho_p VL$ parameter to exceed the elastic limit of the target material. The K factor in equation (5) was quantitatively determined from the slope of the curves for penetration plotted against momentum and is defined as

$$K = K_p K_t \tag{6}$$

where K_p is the projectile deformation factor which accounts for the forces acting on and between the imaginary rods and K_t is the reciprocal of the target resistance factor. Since lead has lower strength properties than any of the materials tested, the value of K_p for lead was arbitrarily chosen as 1. The value of K_t for any target material tested was then equal to K in equation (6) when the projectile material was lead and is simply the slope of the corresponding penetration momentum curve.

The values of K_p for projectile materials other than lead were determined by dividing the resulting value of K by the value of K_t obtained by impacting the same target material with lead projectiles.

Equation (5) is limited to target materials in which the penetration is a linear function of the projectile momentum per unit area. In figure 8, it is shown that the penetration of projectiles into lead targets is not a linear function of momentum and, consequently, cannot be predicted by equation (5). It should be noted, however, that, with

the exception of lead targets, the values of K_p and K_t are constants. By choosing any combination of these constants as listed in table II, the curve may be drawn to approximate the penetration for the desired projectile and target material.

The proposed linear equation of penetration is not limited to the materials tested in this investigation. To predict the penetration resulting from projectile materials listed in table II into target materials other than those tested in this program will only require the impacting of a sufficient number of any of the given material projectiles into the desired target material. If the resulting penetration is linear with respect to the projectile momentum, the value of K_p from table II can be used in equation (6) to determine the value of K_t for the new target material. The penetration can then be predicted for the remaining projectile materials listed in table II since K_p remains constant for the materials tested. This condition would in effect result in four sets of data conditions for the effort expended in obtaining one condition. The constants in table II could very easily be expanded to cover any combinations of projectile and target materials which could be explained by this linear equation.

The fact that lead targets and possibly other target materials do not produce linear curves for the penetration plotted against momentum per unit area does not mean that the penetration is not a function of the momentum per unit area. Rather it indicates that the value of K_t is a variable depending on the impact conditions and is not a constant as with many materials.

Additional research and data are necessary before the resistance of lead to penetration can be explained for a very wide range of impact conditions.

Projectile Mass and Configuration

The previous discussion of the $\rho_p VL$ parameter would indicate that the penetration is independent of the total mass. This independency would infer that a sphere and a cylinder, having the same diameter and a length-diameter ratio of 1, would result in the same penetration. A cylinder having a diameter and a length-diameter ratio of 1 compared with a sphere of the same diameter would have a third greater mass. It can be seen in figures 5 to 8 that cylinders possessing a third more "total momentum" than spheres of the same diameter yielded essentially the same penetration. This result substantiates the conclusion that penetration is not to be correlated with the total momentum of the impacting projectile but as a function of the momentum per unit area.

Equation (5) is not limited to spheres and cylinders but can be applied to projectiles or particles regardless of the configuration, provided the target is semi-infinite with respect to the projectiles.

Correlation of Penetrations in Lead and Copper Targets

A hypothesis has been suggested in reference 1 that the penetrations into targets of different materials could be correlated on the basis of the speed of sound in the target materials. Based upon this assumption, impacts have been made in lead targets at low velocities to simulate impacts into copper at high velocities. The results of this study have been presented in reference 2. For the same impact Mach number in the range presented, the craters in lead and copper appeared to be very similar and the penetrations were reported to be the same.

The results of this present investigation indicate that the correlation between lead and copper targets depends upon factors other than the impact Mach number V/a alone. This correlation was observed when it was first noted that the penetrations varied linearly in copper and nonlinearly in lead. For this reason extreme caution should be exercised in the use of this type of hypothesis until sufficient data are available to substantiate or deny its validity.

Dependence of Penetration on Density and Elastic Properties

The data obtained as a result of this investigation indicated that the penetration was directly affected by the density of the projectile. The magnitude of the penetration into a particular target material by various projectile materials varied in the order shown in figure 9. The figure shows that for an equivalent momentum per unit area the maximum penetration is obtained by the lowest density projectile and decreases in the order of increasing density. If a material is desired for optimum design of projectiles of a fixed diameter such that the projectile can achieve the maximum penetration per projectile weight, it appears that the lowest density material should be used. It is observed from figure 9 that, as the value of K_p increases for various materials, the penetration increases accordingly. This result would indicate that the value of K_p is inversely proportional to the density of the projectile.

Analysis of the data for a particular projectile material and varying target materials indicated that the penetrations were greater

in target materials having the lowest modulus of elasticity when plotted against the $\rho_p VL$ parameter. This relationship is shown in figure 10.

From this figure it is observed that, as the penetration increases for various materials, the value of K_t increases accordingly. Thus, the value of K_t is inversely proportional to the modulus of elasticity of the target.

Figures 9 and 10 indicate that the maximum penetration for a specific quantity of momentum per unit area is obtained by impacting a low-density projectile into a target having a low modulus of elasticity.

L 7 6 6

Crater Diameters

The ratio of crater diameter to projectile diameter was plotted as a function of velocity and presented in figures 11 to 14. Since target penetration was the primary purpose of this investigation, the measured data have been presented and no attempt was made to define a curve through the data points. However, as a matter of convenience for anyone interested in these parameters, the data are available in figures 11 to 14 and in tabular form in table I. A brief study of these data indicated that the ratio of crater diameter to projectile diameter increased with increasing velocity and was independent of the projectile size or configuration within the scope of this investigation.

Crater Volume

The crater volumes were plotted against the "effective kinetic energy" of the projectile and are presented in figures 15 to 18. The "effective kinetic energy" is defined as that quantity of energy available to produce cratering. As was observed in the plots of penetration against momentum per unit area, the projectile must possess a certain amount of energy before cratering effects are observed.

The data results indicated that a projectile must possess at least 50 foot-pounds of kinetic energy in order to produce permanent deformation in aluminum and steel targets. Lead and copper targets did not exhibit this resistance and the curves faired through the data points appeared to pass through the origin when plotted on regular graph paper.

The data appeared to be defined approximately by the equation

$$v = A(\text{Effective kinetic energy}) \qquad (7a)$$

or

$$v = A\left(\frac{1}{2} mV^2 - B\right) \tag{7b}$$

where B is that quantity of energy necessary to produce cratering and A is a constant of proportionality.

The value of A in equation (7) depends upon the material used for the projectile and target and is defined as

$$A = A_p A_t \tag{8}$$

where A_p is a factor describing the projectile and A_t is the reciprocal of target resistance. It is noted that, as the target strength or resistance increases, the value of A_t decreases; thus, the crater volume for a projectile possessing a given quantity of kinetic energy is reduced. The value of these constants is listed in table II for the materials tested in this investigation. Thus, 16 combinations of target and projectile materials may be used to predict the crater volumes resulting from their high-velocity impacts. The predicted crater volumes resulting from the impact of the projectile materials listed in table II may be obtained for any target material provided the crater volumes are a linear function of kinetic energy. The crater volumes would be obtained in the same manner as described previously for predicting penetrations into targets not tested in this investigation. From the one set of data obtained by this method, the volumes could be predicted for three other conditions. This method would require a sufficient number of projectiles to determine the linearity of the data and the determination of A_t from equation (8).

It should be noted that the data in figures 15 to 18 have been plotted on logarithmic 3 × 3 cycle graph paper. This type of plot was necessary to cover adequately the wide range of impact conditions. This type of plot also readily points out the dependence of crater volumes on the strength and speed of sound of the target materials. The greater volumes were obtained in the target having the lowest strength and lowest speed of sound and decreased proportionately as the strength and speed of sound were increased in the target material.

It is observed from figure 19 that all craters with the exception of those in aluminum were very nearly hemispherical. The craters in aluminum were irregular and slightly pointed. Craters in lead and copper targets were similar to the hemispherical crater shown for steel.

It is noted from table I that the volumes of only a small percentage of the total number of projectiles were obtained. This lack of volume data was due to the projectile being imbedded in the target or

the crater being lined with the projectile material. In the latter case, it appeared that the projectile flowed plastically during the time interval of impact. In measuring the penetration in these craters, the crater was either cross sectioned or a hole drilled in the bottom of the crater to the target material. There were, however, a sufficient number of craters in which the volume could be obtained reliably and these data are listed in table I and shown graphically in figures 15 to 18.

CONCLUDING REMARKS

It has been shown that the penetration of high-velocity metal projectiles of aluminum, copper, lead, and steel into aluminum, copper, and steel targets can be correlated as a function of the maximum momentum per unit area possessed by the projectile. This momentum per unit area is defined as the product of projectile density, velocity, and effective length. If this product is kept constant for a given projectile material into a given target, the depth of penetration will also remain constant regardless of what the total projectile momentum or kinetic energy may be.

For the case of aluminum, copper, and steel targets, the penetration proved to be a linear function of momentum per unit area. The lead targets impacted produced a nonlinear curve of penetration plotted against momentum per unit area. It is evident from this plot that the resistance of lead to penetration is a function of the impact conditions rather than being a constant function of momentum per unit area as indicated by the other materials tested. Although many of the impacts in lead targets were at velocities above the speed of sound, the penetration curves were continuous and showed no abrupt change in the resistance in the impact Mach number 1 region. This continuity indicates that the resistance of the other metals should continue to be a constant regardless of velocity and that the equations given for penetration will hold true for impact velocities greater than a Mach number of 1.

The crater volumes were found to be a linear function of the total kinetic energy possessed by the projectile, the largest craters being found in the target material having the lowest strength and the lowest speed of sound.

Langley Research Center,
National Aeronautics and Space Administration,
Langley Field, Va., December 14, 1959.

REFERENCES

1. Huth, J. H., Thompson, J. S., and Van Valkenburg, M. E.: Some New Data on High-Speed Impact Phenomena. Jour. Appl. Mech., vol. 24, no. 1, Mar. 1957, pp. 65-68.

2. Charters, A. C., Jr., and Locke, G. S., Jr.: A Preliminary Investigation of High-Speed Impact: The Penetration of Small Spheres Into Thick Copper Targets. NACA RM A58B26, 1958.

3. Kinard, William H., and Lambert, C. H., Jr.: An Investigation of the Effect of Target Temperature on Projectile Penetration and Cratering. NACA RM L58E14, 1958.

4. Van Fleet, H. B., Whited, C. R., and Partridge, W. S.: High Velocity Impact Craters in Lead-Tin Alloys. Tech. Rep. OSR-13 (AFOSR-TN-58-28, Contract No. AF 18(600)1217), Dept. Elec. Eng., Univ. of Utah, Jan. 1958. (Available as ASTIA Doc. AD 148067.)

TABLE I.- HIGH-VELOCITY IMPACT DATA

Projectile	Projectile material	Target material	Velocity, fps	Penetration, in.	Crater diameter, in.	Crater volume, cu in.
0.22-inch-diameter sphere						
1	Copper	Copper	1,481	0.110	0.27	------
2	Copper	Copper	2,230	.142	.29	------
3	Copper	Copper	3,130	.184	.37	------
4	Copper	Copper	3,770	.208	.42	------
5	Copper	Copper	4,320	.235	.46	------
6	Copper	Copper	4,860	.258	.51	------
7	Copper	Copper	5,190	.272	.52	------
8	Steel	Copper	1,220	.102	.21	0.0023
9	Steel	Copper	2,405	.164	.28	------
10	Steel	Copper	3,250	.210	.33	------
11	Steel	Copper	3,800	.234	.37	------
12	Steel	Copper	4,680	.282	.42	------
13	Steel	Copper	4,860	.291	.42	------
14	Steel	Copper	5,380	.315	.46	------
15	Lead	Copper	1,218	.093	.29	.0039
16	Lead	Copper	1,800	.143	.32	.0104
17	Lead	Copper	2,520	.199	.36	.0159
18	Lead	Copper	3,315	.233	.38	.0216
19	Lead	Copper	3,560	.255	.40	.0255
20	Lead	Copper	3,675	.250	.38	.0211
21	Lead	Copper	3,980	.285	.39	.028
22	Aluminum	Copper	1,079	.034	.18	.0005
23	Aluminum	Copper	2,242	.060	.25	.0016
24	Aluminum	Copper	3,470	.091	.30	.0034
25	Aluminum	Copper	4,180	.106	.32	.0051
26	Aluminum	Copper	4,980	.120	.36	.0069
27	Aluminum	Copper	5,285	.127	.37	.0074
28	Aluminum	Copper	6,260	.150	.40	.0099
29	Copper	Aluminum	1,500	.060	.26	------
30	Copper	Aluminum	2,275	.120	.23	------
31	Copper	Aluminum	3,070	.186	.29	------
32	Copper	Aluminum	3,640	.248	.32	------
33	Copper	Aluminum	4,230	.295	.32	------
34	Copper	Aluminum	5,050	.375	.37	------
35	Copper	Aluminum	5,310	.397	.38	------
36	Steel	Aluminum	1,136	.071	----	------
37	Steel	Aluminum	2,040	.131	----	------
38	Steel	Aluminum	3,140	.195	----	------
39	Steel	Aluminum	3,875	.250	----	------
40	Steel	Aluminum	4,520	.276	----	------
41	Steel	Aluminum	5,020	.316	----	------
42	Steel	Aluminum	5,420	.334	----	------
43	Lead	Aluminum	1,232	.045	----	------
44	Lead	Aluminum	1,382	.075	----	------
45	Lead	Aluminum	2,080	.140	----	------
46	Lead	Aluminum	2,480	.200	----	------
47	Lead	Aluminum	3,430	.270	----	------
48	Lead	Aluminum	3,820	.275	----	------
49	Lead	Aluminum	4,000	.290	----	------
50	Aluminum	Aluminum	1,248	.010	----	------
51	Aluminum	Aluminum	2,380	.040	----	------
52	Aluminum	Aluminum	3,455	.064	----	------
53	Aluminum	Aluminum	4,310	.080	----	------
54	Aluminum	Aluminum	5,000	.110	----	------
55	Aluminum	Aluminum	6,140	.135	----	------
56	Aluminum	Aluminum	6,550	.162	----	------

TABLE I.- HIGH-VELOCITY IMPACT DATA - Continued

Projectile	Projectile material	Target material	Velocity, fps	Penetration, in.	Crater diameter, in.	Crater volume, cu in.
0.22-inch-diameter sphere						
57	Copper	Steel	727	0.009	0.13	-------
58	Copper	Steel	2,100	.052	.28	0.0016
59	Copper	Steel	2,780	.107	.32	.0042
60	Copper	Steel	3,630	.118	.33	-------
61	Copper	Steel	4,170	.145	.36	-------
62	Copper	Steel	4,780	.169	.38	-------
63	Copper	Steel	5,250	.190	.42	-------
64	Steel	Steel	1,035	.020	.16	-------
65	Steel	Steel	2,070	.055	.26	-------
66	Steel	Steel	2,680	.090	.29	-------
67	Steel	Steel	3,690	.126	.33	-------
68	Steel	Steel	4,440	.152	.34	-------
69	Steel	Steel	4,970	.165	.36	-------
70	Steel	Steel	5,520	.180	.38	-------
71	Lead	Steel	856	.012	.16	-------
72	Lead	Steel	1,375	.045	.29	-------
73	Lead	Steel	3,160	.097	.31	-------
74	Lead	Steel	3,140	.101	.35	-------
75	Lead	Steel	3,360	.124	.30	-------
76	Lead	Steel	3,960	.162	.33	-------
77	Lead	Steel	4,220	.187	.37	-------
78	Aluminum	Steel	444	0	0	-------
79	Aluminum	Steel	2,050	.009	.15	-------
80	Aluminum	Steel	2,880	.025	.19	-------
81	Aluminum	Steel	3,740	.035	.25	.00046
82	Aluminum	Steel	4,610	.049	.30	.00069
83	Aluminum	Steel	5,820	.063	.33	.00299
84	Aluminum	Steel	6,460	.075	.35	.00391
85	Copper	Lead	1,410	.277	.38	.0202
86	Copper	Lead	2,320	.363	.53	.0471
87	Copper	Lead	3,100	.431	.64	.0745
88	Copper	Lead	3,540	.432	.71	.099
89	Copper	Lead	4,000	.465	.84	.1538
90	Copper	Lead	4,880	.556	.87	.194
91	Copper	Lead	5,410	.510	.95	.213
92	Steel	Lead	1,135	.323	.28	.0113
93	Steel	Lead	1,990	.383	.44	.0303
94	Steel	Lead	2,910	.424	.58	.0595
95	Steel	Lead	3,640	.488	.68	.094
96	Steel	Lead	4,370	.551	.74	.125
97	Steel	Lead	5,000	.572	.83	.163
98	Steel	Lead	-----	-----	----	.186
99	Lead	Lead	1,368	.246	.43	.0252
100	Lead	Lead	2,010	.297	.58	.0512
101	Lead	Lead	2,690	.351	.67	.0834
102	Lead	Lead	3,250	.421	.77	.1225
103	Lead	Lead	3,670	.460	.80	.1455
104	Lead	Lead	3,980	.461	.82	.156
105	Lead	Lead	4,180	.498	.87	.185
106	Aluminum	Lead	1,570	.109	.24	.0032
107	Aluminum	Lead	1,355	.108	.26	.0039
108	Aluminum	Lead	2,920	.154	.39	.0117
109	Aluminum	Lead	4,000	.208	.47	.020
110	Aluminum	Lead	4,630	.219	.52	.0285
111	Aluminum	Lead	5,380	.233	.54	.0368
112	Aluminum	Lead	6,030	.246	.56	.0437

TABLE I.- HIGH-VELOCITY IMPACT DATA - Continued

Projectile	Projectile material	Target material	Velocity, fps	Penetration, in.	Crater diameter, in.	Crater volume, cu in.
0.22-inch-diameter cylinder L/d = 1						
113	Copper	Copper	1,150	0.084	0.28	0.0039
114	Copper	Copper	2,050	.161	.32	.0104
115	Copper	Copper	2,790	.229	.38	.0182
116	Copper	Copper	3,290	.261	.45	.0277
117	Copper	Copper	3,960	.302	.50	.0388
118	Copper	Copper	4,390	.306	.50	.0404
119	Copper	Copper	4,690	.354	.56	.0556
120	Steel	Copper	922	.051	.22	.0017
121	Steel	Copper	2,242	.156	.33	.0101
122	Steel	Copper	2,940	.201	.37	------
123	Steel	Copper	3,750	.279	.42	.0269
124	Steel	Copper	4,200	.299	.47	------
125	Steel	Copper	4,630	.330	.50	------
126	Steel	Copper	5,140	.341	.52	------
127	Lead	Copper	1,240	.084	.27	------
128	Lead	Copper	1,590	.134	.37	------
129	Lead	Copper	2,560	.216	.40	------
130	Lead	Copper	2,940	.228	.41	------
131	Lead	Copper	3,495	.269	.43	------
132	Lead	Copper	3,520	.268	.43	------
133	Lead	Copper	4,110	.293	.46	------
134	Aluminum	Copper	1,052	.019	.23	------
135	Aluminum	Copper	2,190	.057	.26	------
136	Aluminum	Copper	2,960	.102	.33	------
137	Aluminum	Copper	3,980	.116	.38	------
138	Aluminum	Copper	4,900	.135	.40	------
139	Aluminum	Copper	5,080	.143	.42	------
140	Aluminum	Copper	5,660	.168	.44	------
141	Copper	Aluminum	1,335	.037	.25	.0025
142	Copper	Aluminum	2,080	.102	.32	.0058
143	Copper	Aluminum	2,600	.170	.33	.0113
144	Copper	Aluminum	3,150	.244	.33	.0166
145	Copper	Aluminum	3,940	.300	.35	.0230
146	Copper	Aluminum	4,540	.331	.37	.0331
147	Copper	Aluminum	4,740	.423	.37	.0336
148	Steel	Aluminum	1,235	.049	.23	.0014
149	Steel	Aluminum	1,960	.102	.25	.0044
150	Steel	Aluminum	2,910	.165	.30	.0094
151	Steel	Aluminum	3,520	.218	.33	.0154
152	Steel	Aluminum	4,200	.285	.34	.0214
153	Steel	Aluminum	4,740	.346	.36	.0283
154	Steel	Aluminum	5,180	.400	.37	.0301
155	Lead	Aluminum	1,285	.029	.25	.0028
156	Lead	Aluminum	1,980	.107	.34	.0062
157	Lead	Aluminum	2,440	.192	.30	.0102
158	Lead	Aluminum	2,930	.206	.33	.0131
159	Lead	Aluminum	3,370	.296	.29	.0177
160	Lead	Aluminum	3,800	.325	.33	.0209
161	Lead	Aluminum	4,830	.351	.34	------
162	Aluminum	Aluminum	1,370	.010	----	------
163	Aluminum	Aluminum	2,400	.040	.24	.0007
164	Aluminum	Aluminum	2,880	.048	.27	.0012
165	Aluminum	Aluminum	4,000	.086	.32	.0044
166	Aluminum	Aluminum	4,620	.112	.35	.0060
167	Aluminum	Aluminum	5,090	.121	.38	.0085
168	Aluminum	Aluminum	6,320	.153	.42	.0134

TABLE I.- HIGH-VELOCITY IMPACT DATA - Continued

Projectile	Projectile material	Target material	Velocity, fps	Penetration, in.	Crater diameter, in.	Crater volume, cu in.
0.22-inch-diameter cylinder L/d = 1						
169	Copper	Steel	1,005	0.009	0.22	------
170	Copper	Steel	2,050	.051	.31	0.0021
171	Copper	Steel	2,530	.081	.34	.0041
172	Copper	Steel	3,600	.122	.41	.0110
173	Copper	Steel	3,950	.145	.42	.0131
174	Copper	Steel	4,640	.167	.45	.0197
175	Copper	Steel	4,750	.179	.46	.020
176	Steel	Steel	1,120	.010	.22	------
177	Steel	Steel	2,220	.037	.29	.0025
178	Steel	Steel	2,935	.095	.33	.0048
179	Steel	Steel	3,550	.120	.37	------
180	Steel	Steel	4,110	.140	.39	------
181	Steel	Steel	4,810	.175	.42	------
182	Steel	Steel	5,080	.208	.44	------
183	Lead	Steel	1,270	.012	.22	------
184	Lead	Steel	1,295	.052	.34	------
185	Lead	Steel	1,585	.050	.35	------
186	Lead	Steel	2,925	.105	.37	------
187	Lead	Steel	3,400	.145	.37	------
188	Lead	Steel	3,790	.164	.41	.0108
189	Lead	Steel	4,060	.195	.39	------
190	Aluminum	Steel	1,130	0	----	------
191	Aluminum	Steel	2,210	.011	.22	------
192	Aluminum	Steel	3,240	.025	.25	.0006
193	Aluminum	Steel	3,800	.033	.28	.0012
194	Aluminum	Steel	4,660	.051	.33	.0023
195	Aluminum	Steel	5,680	.082	.36	.0044
196	Aluminum	Steel	6,390	.085	.38	.0053
197	Copper	Lead	1,220	.236	.41	.0221
198	Copper	Lead	2,320	.482	.61	.0838
199	Copper	Lead	2,990	.476	.74	.1248
200	Copper	Lead	3,550	.506	.85	.172
201	Copper	Lead	4,020	.540	.95	.233
202	Copper	Lead	4,450	.565	.99	.268
203	Copper	Lead	5,000	.586	1.06	.322
204	Steel	Lead	1,052	.177	.37	.0133
205	Steel	Lead	2,250	.372	.54	.053
206	Steel	Lead	3,080	.503	.67	.101
207	Steel	Lead	3,860	.560	.79	.1415
208	Steel	Lead	4,250	..569	.80	.1815
209	Steel	Lead	4,780	.573	.93	.223
210	Steel	Lead	5,210	.582	1.02	.276
211	Lead	Lead	1,250	.246	----	.0292
212	Lead	Lead	1,945	.357	.67	.0756
213	Lead	Lead	2,500	.423	.73	.118
214	Lead	Lead	3,020	.453	.78	.139
215	Lead	Lead	3,470	.467	.87	.177
216	Lead	Lead	4,020	.497	.88	.224
217	Lead	Lead	4,220	.491	.89	.201
218	Aluminum	Lead	1,120	.070	.29	.0031
219	Aluminum	Lead	2,180	.138	.39	.0106
220	Aluminum	Lead	3,230	.204	.46	.020
221	Aluminum	Lead	4,170	.220	.58	.0292
222	Aluminum	Lead	4,780	.241	.61	.0384
223	Aluminum	Lead	5,460	.261	.63	.0476
224	Aluminum	Lead	6,290	.288	----	.0623

TABLE I.- HIGH-VELOCITY IMPACT DATA - Concluded

Projectile	Projectile material	Target material	Velocity, fps	Penetration, in.	Crater diameter, in.	Crater volume, cu in.
0.50-inch-diameter cylinder L/d = 1						
225	Steel	Aluminum	2,710	0.395	0.73	0.121
226	Steel	Aluminum	4,040	.750	----	------
227	Steel	Aluminum	4,880	.880	.94	.434
228	Aluminum	Aluminum	3,270	.190	.72	.0414
229	Aluminum	Aluminum	5,330	.343	.91	.1285
230	Aluminum	Aluminum	6,450	.610	.95	.243
231	Copper	Aluminum	2,590	.400	.74	.129
232	Copper	Aluminum	3,830	.830	.86	.333
233	Copper	Aluminum	4,650	1.108	.97	.480
234	Lead	Aluminum	-----	-----	----	------
235	Lead	Aluminum	3,300	.770	.75	.263
236	Lead	Aluminum	4,070	.945	.82	.431
237	Lead	Steel	2,300	.175	.82	.0528
238	Lead	Steel	3,350	.325	.87	------
239	Lead	Steel	4,130	.410	----	------
240	Steel	Copper	2,630	.400	.85	.181
241	Steel	Copper	3,900	.607	1.07	.380
242	Steel	Copper	4,850	.700	1.13	.594
243	Aluminum	Copper	3,360	.195	.82	.069
244	Aluminum	Copper	5,300	.335	1.03	.167
245	Aluminum	Copper	6,500	.405	1.06	.211
256	Lead	Copper	2,255	.415	----	.426
247	Lead	Copper	3,250	.600	1.07	.462
248	Lead	Copper	3,690	.645	1.14	------
0.50-inch-diameter sphere						
249	Steel	Steel	2,400	0.296	0.51	0.0453
250	Steel	Steel	3,595	.399	.72	.074
251	Steel	Steel	4,440	.416	.78	.126
252	Steel	Steel	5,090	.475	.85	.163
253	Steel	Steel	5,610	.500	.89	.194
254	Copper	Steel	2,250	.160	.66	.038
255	Copper	Steel	3,430	.324	.78	.088
256	Copper	Steel	4,230	.413	.89	.133
257	Copper	Steel	-----	.471	.93	------
258	Copper	Steel	5,370	.475	.97	------
259	Aluminum	Steel	2,430	.035	.43	------
260	Aluminum	Steel	4,410	.100	.67	------
261	Aluminum	Steel	5,530	.115	.73	------
262	Aluminum	Steel	6,230	.190	.78	------
263	Aluminum	Steel	7,190	.209	.82	------
264	Copper	Copper	3,480	.54	.88	------
265	Copper	Copper	4,280	.575	1.03	------
266	Copper	Copper	4,980	.710	1.07	------
267	Copper	Copper	5,350	.733	----	------
0.0620-inch-diameter sphere						
268	Steel	Lead	1,510	0.141	0.10	------
269	Steel	Lead	3,620	.136	.19	------
270	Steel	Lead	4,760	.155	.22	------
271	Steel	Lead	6,620	.146	.29	------
272	Aluminum	Lead	1,410	.0415	.07	------
273	Aluminum	Lead	3,620	.051	.12	------
274	Aluminum	Lead	4,760	.067	.13	------
275	Aluminum	Lead	5,780	.064	.16	------
276	Steel	Steel	8,880	.085	----	------
277	Aluminum	Steel	12,500	.028	----	------
278	Steel	Aluminum	5,870	.083	----	------
279	Aluminum	Aluminum	13,200	.086	----	------
280	Steel	Copper	3,950	.090	----	------
281	Aluminum	Copper	13,000	.070	----	------

TABLE II.- CONSTANTS USED IN CRATERING EQUATIONS

Material	K_t	K_p	A_p	A_t	C	B
Copper	0.028	1.10	1.97	34×10^{-6}	0	0
Steel	.017	1.26	1.73	11	1.3	50
Aluminum	.036	1.49	1.00	25	1.3	50
Lead	*	1.00	1.60	162	0	0

*Not constant.

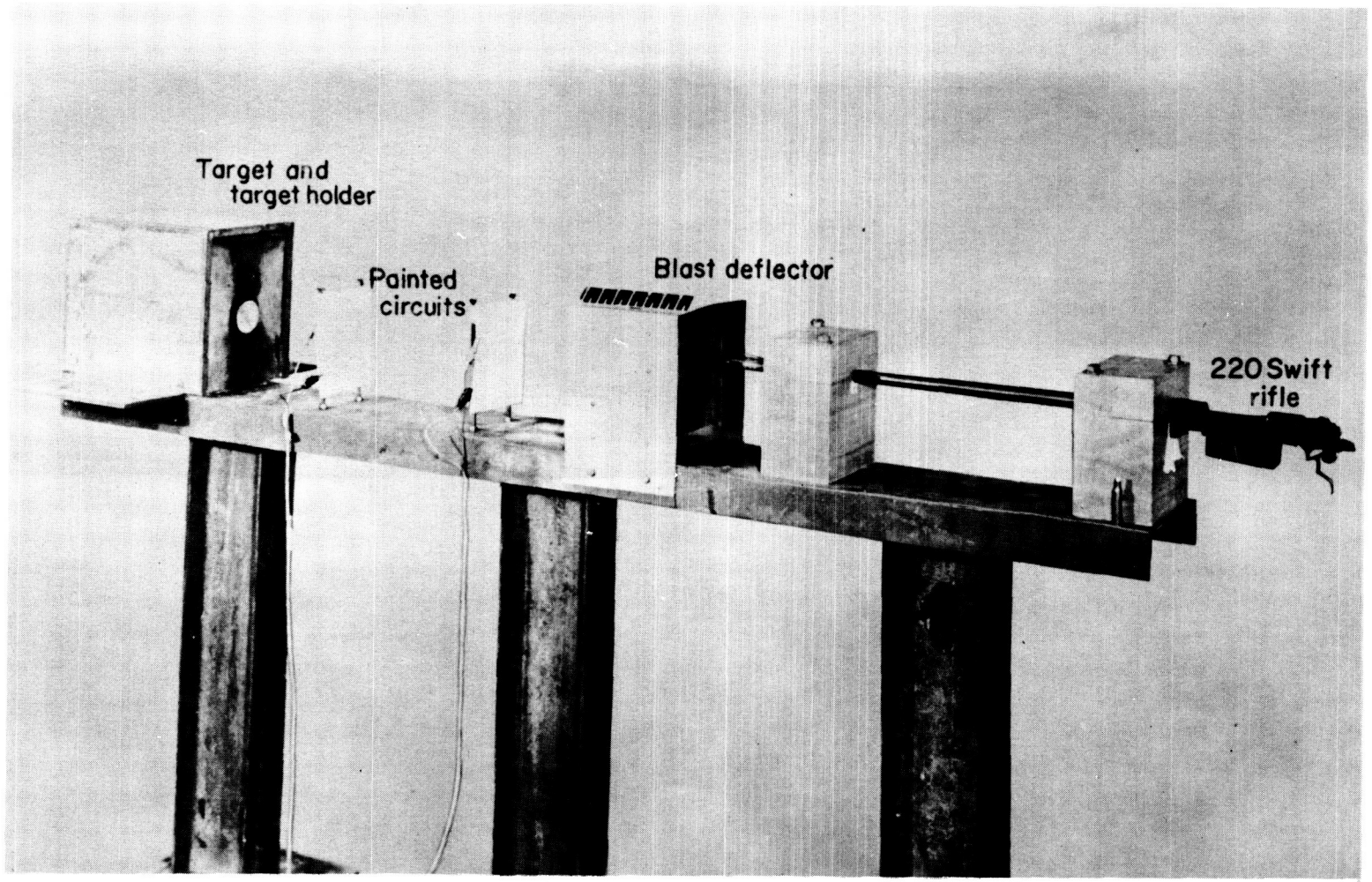

L-57-3298.1

Figure 1.- General arrangement of 220 Swift rifle used in making impact studies.

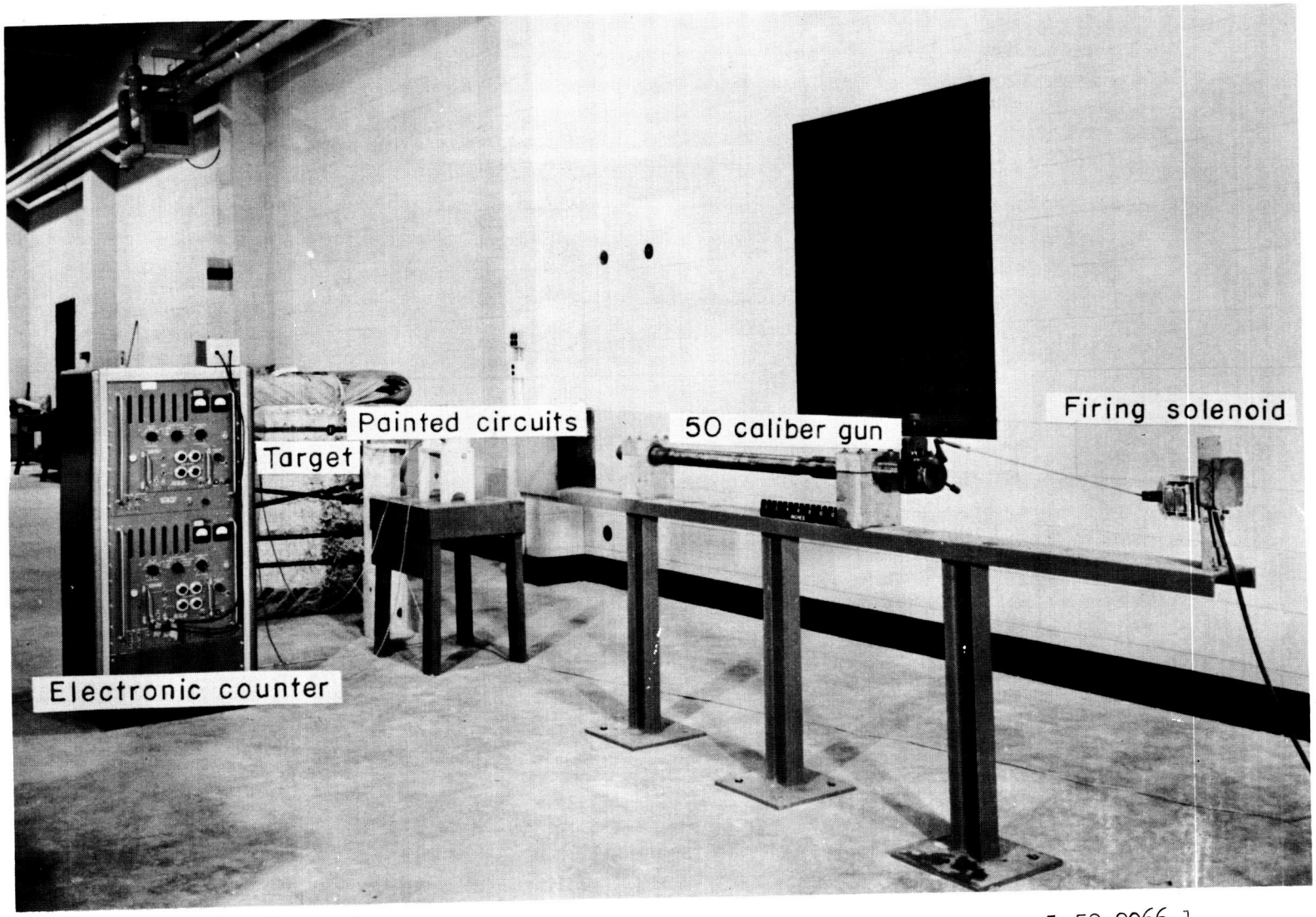

L-59-2066.1

Figure 2.- General arrangement of 50-caliber gun used in making impact studies.

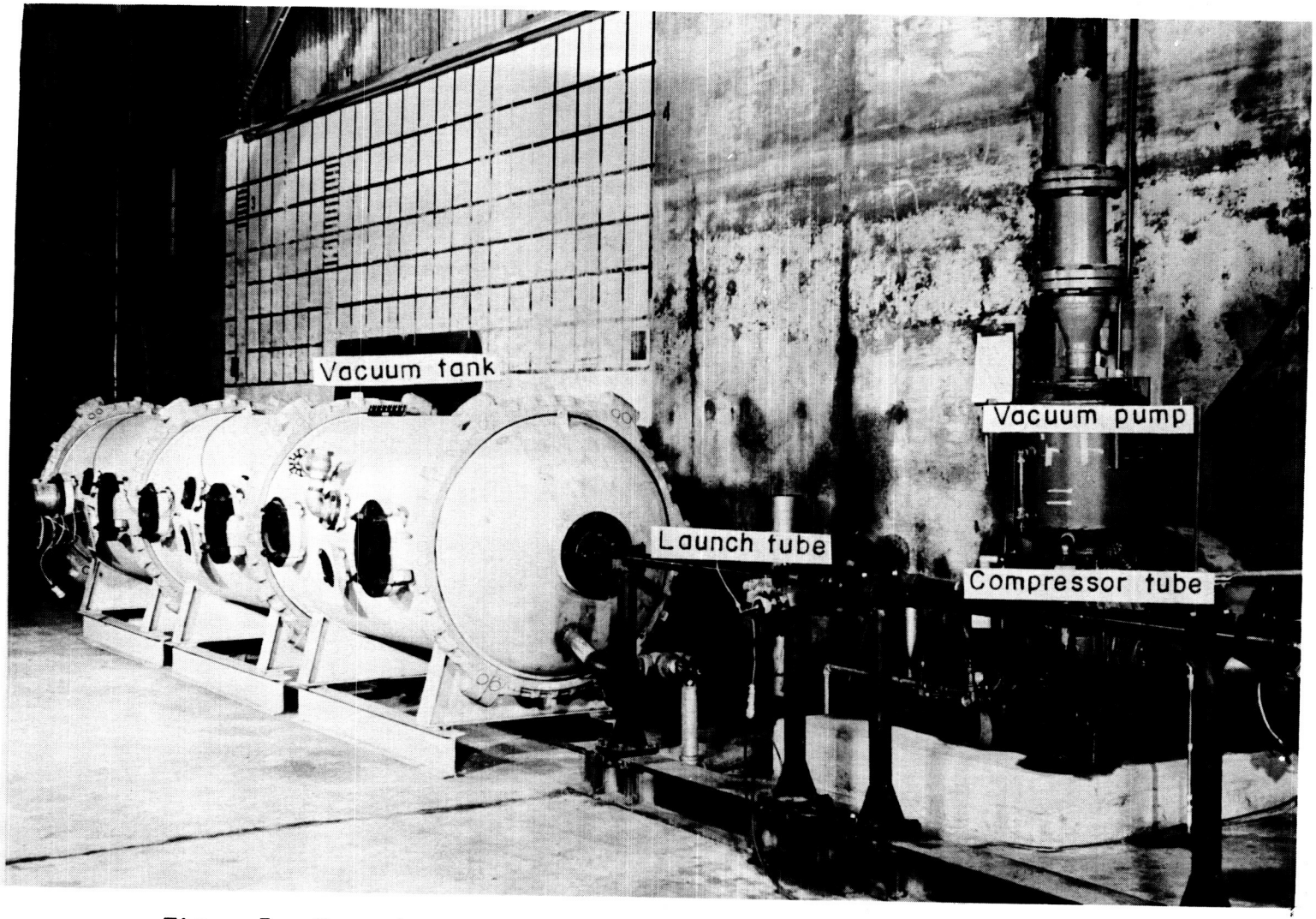

Figure 3.- General arrangement of light-gas gun installation. L-59-2710.1

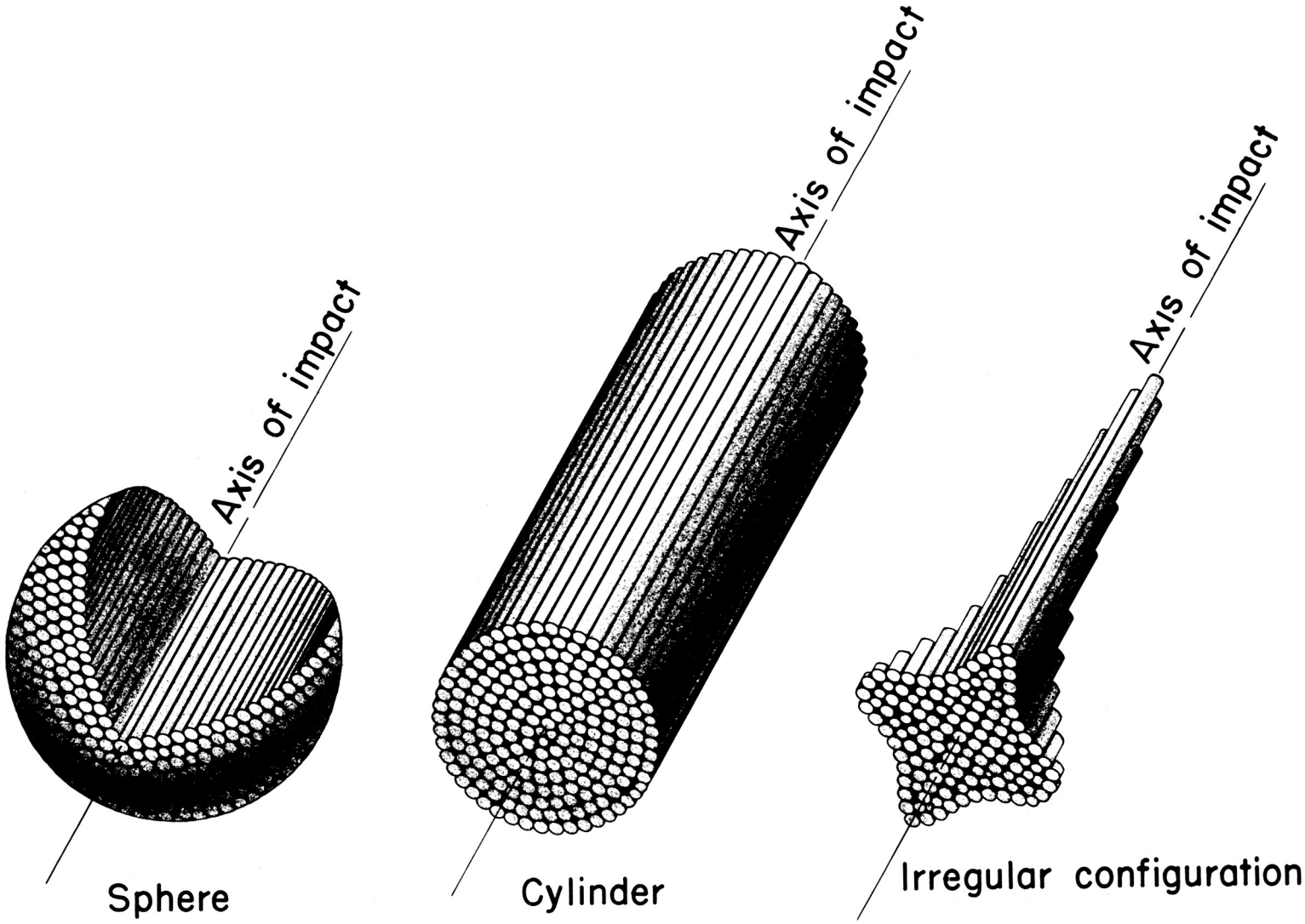

Figure 4.- Projectiles consisting of an infinite number of imaginary rods alined along the path of projectile travel.

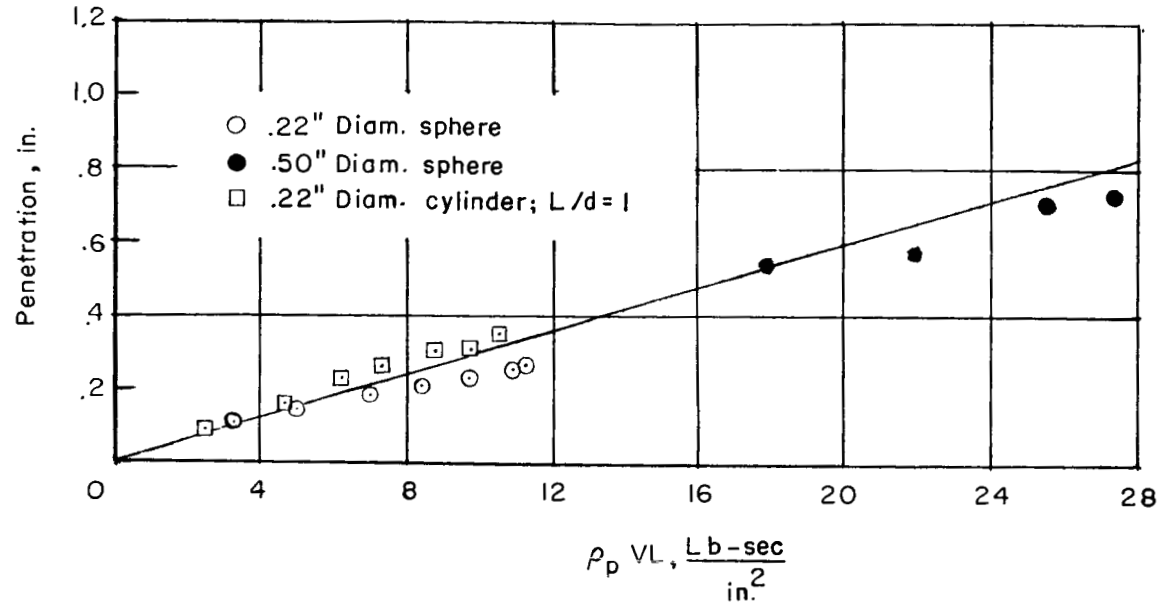

(a) Copper projectile.

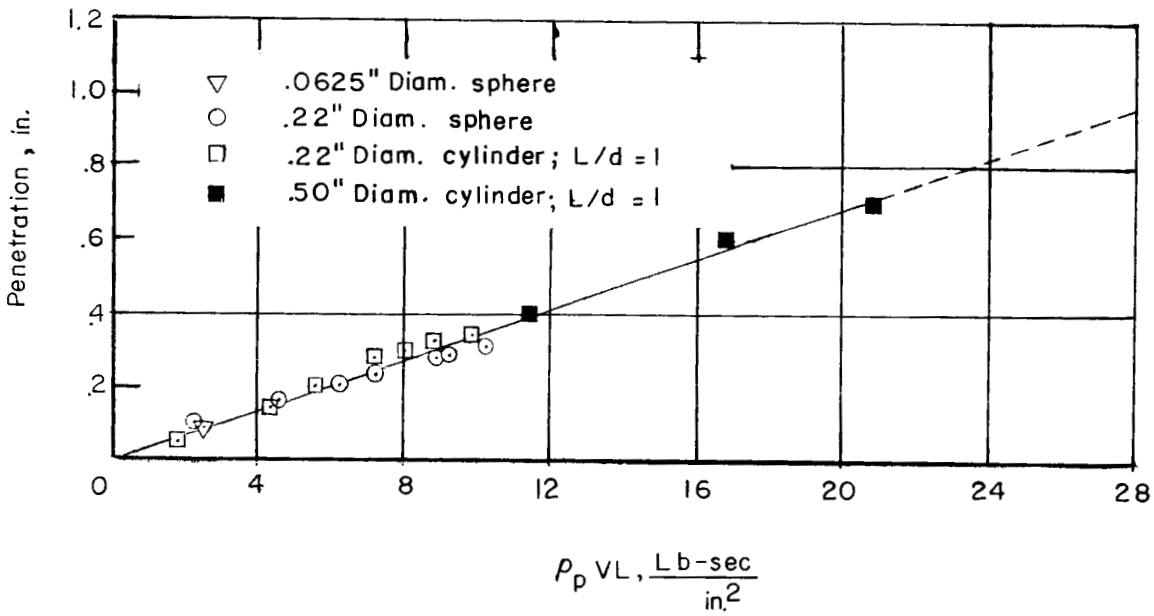

(b) Steel projectile.

Figure 5.- Penetration in copper target plotted against momentum per unit area of impacting projectile.

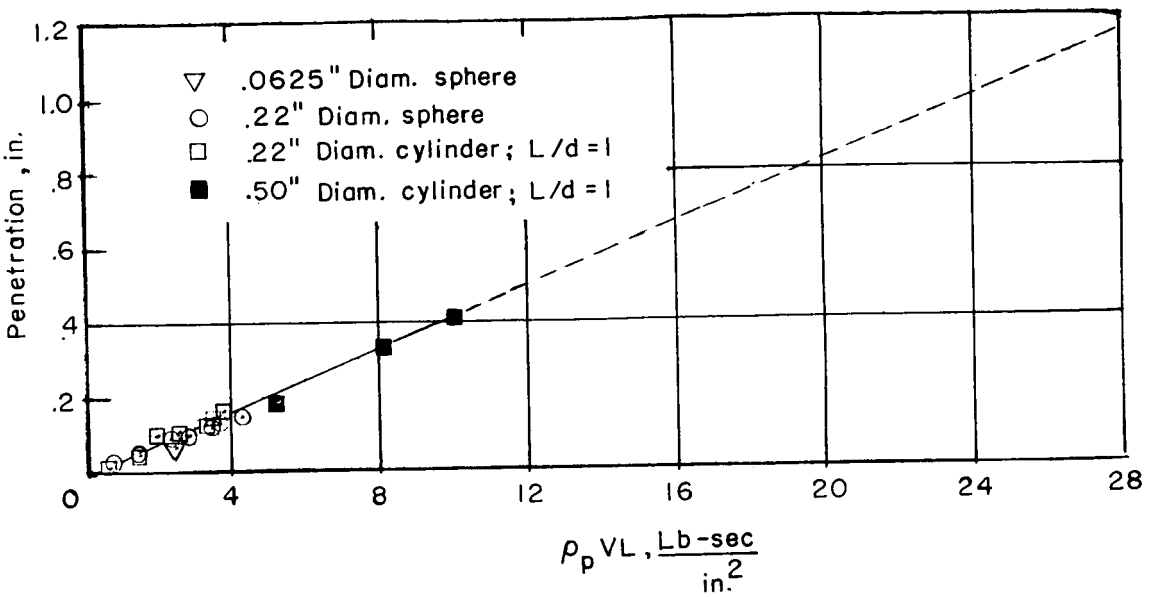

(c) Aluminum projectile.

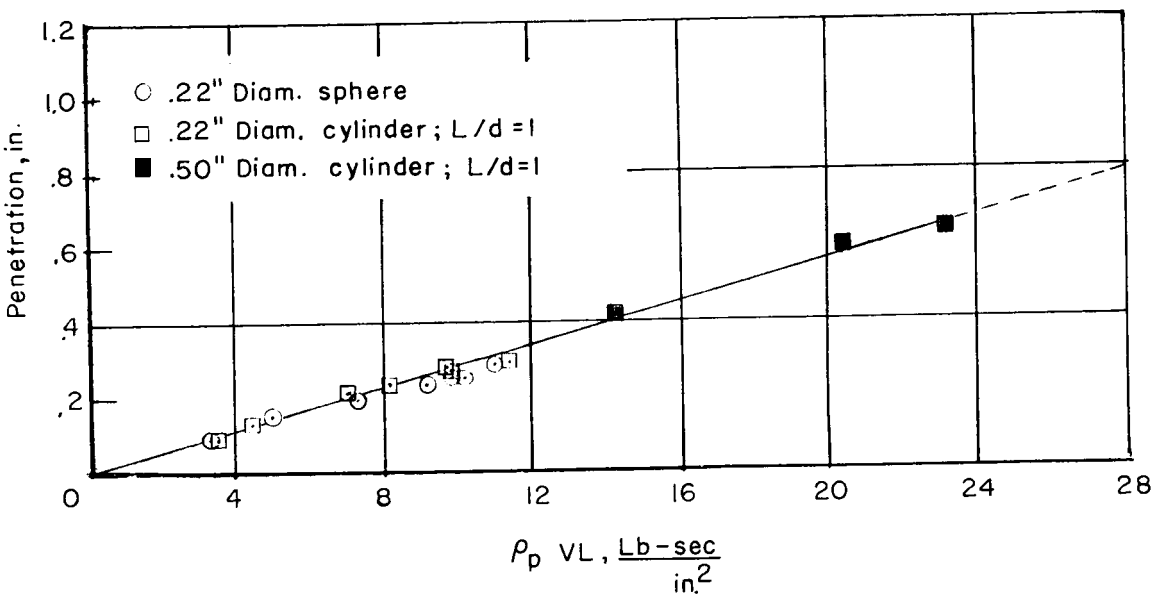

(d) Lead projectile.

Figure 5.- Concluded.

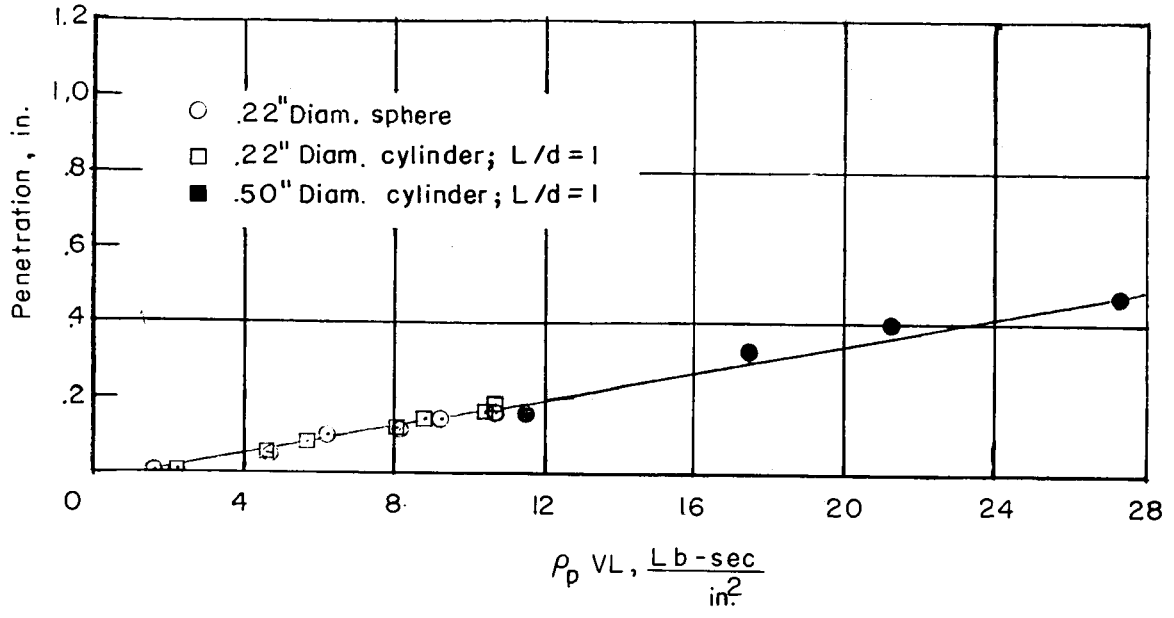

(a) Copper projectile.

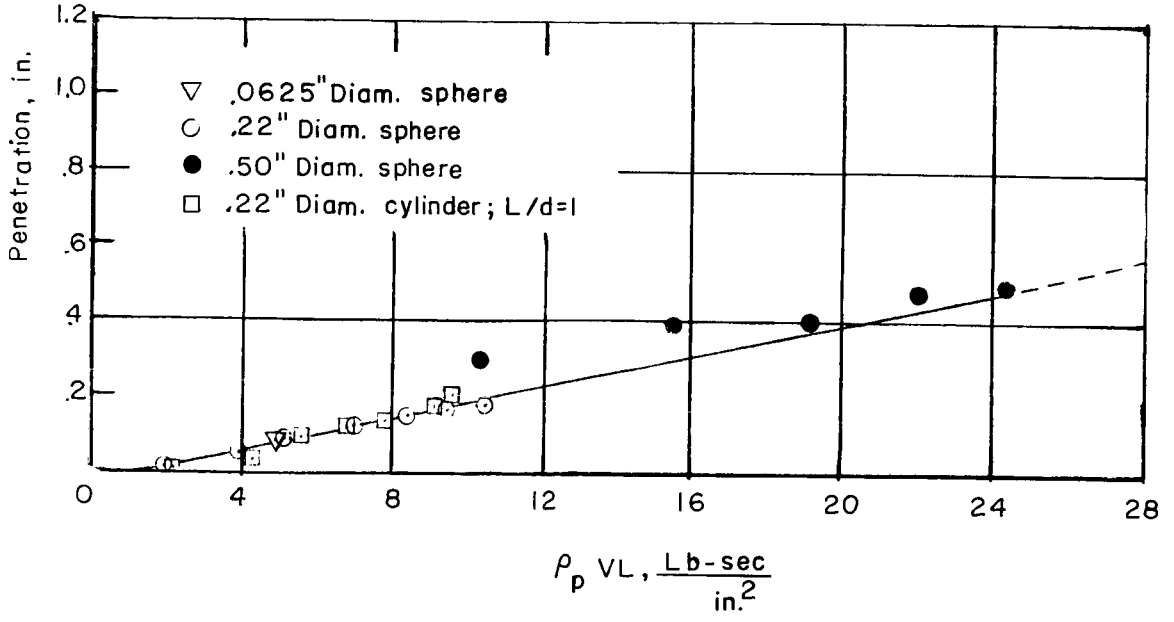

(b) Steel projectile.

Figure 6.- Penetration in steel target plotted against momentum per unit area of impacting projectile.

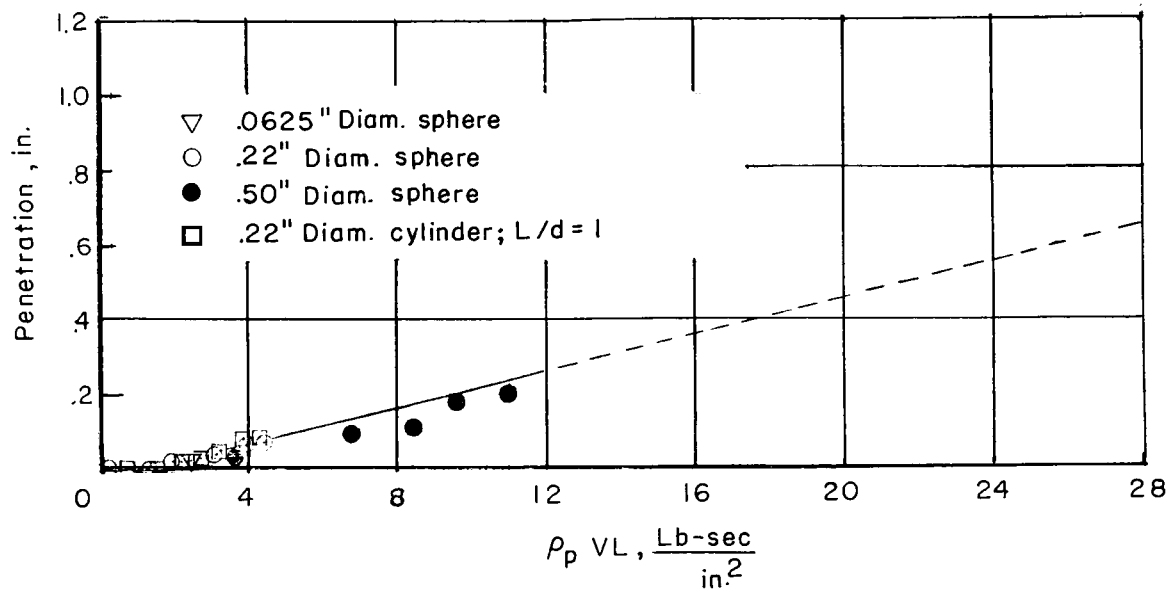

(c) Aluminum projectile.

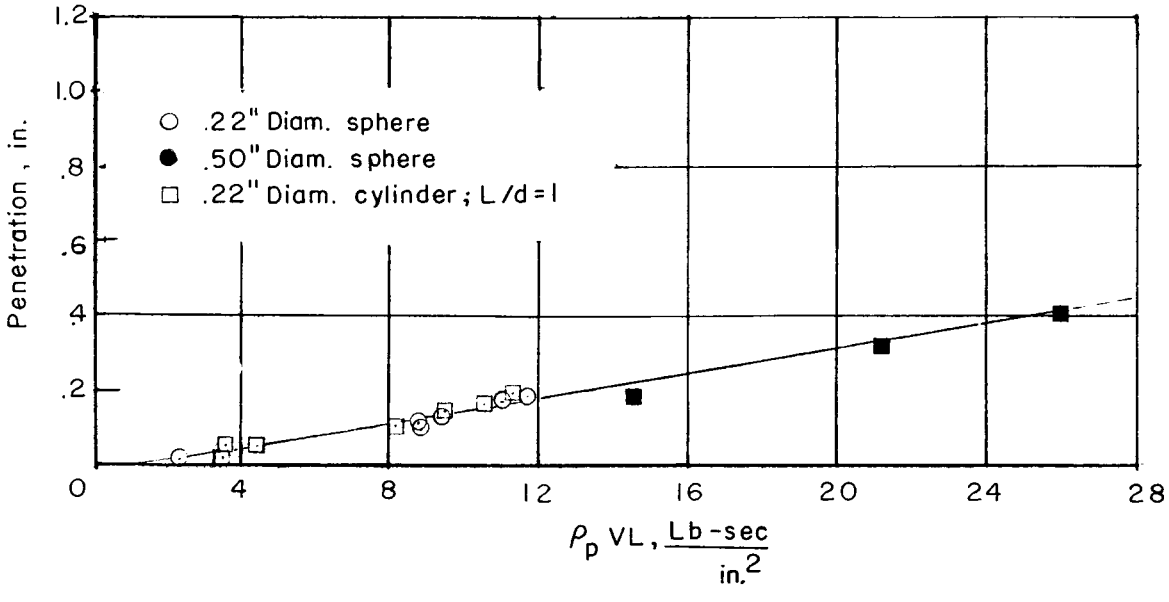

(d) Lead projectile.

Figure 6.- Concluded.

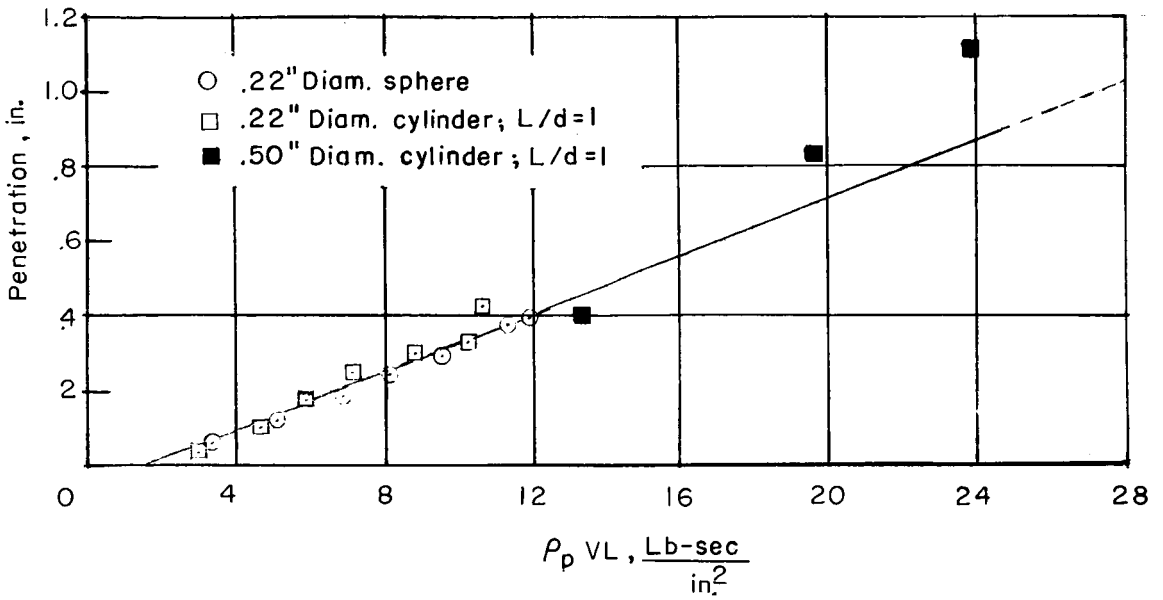

(a) Copper projectile.

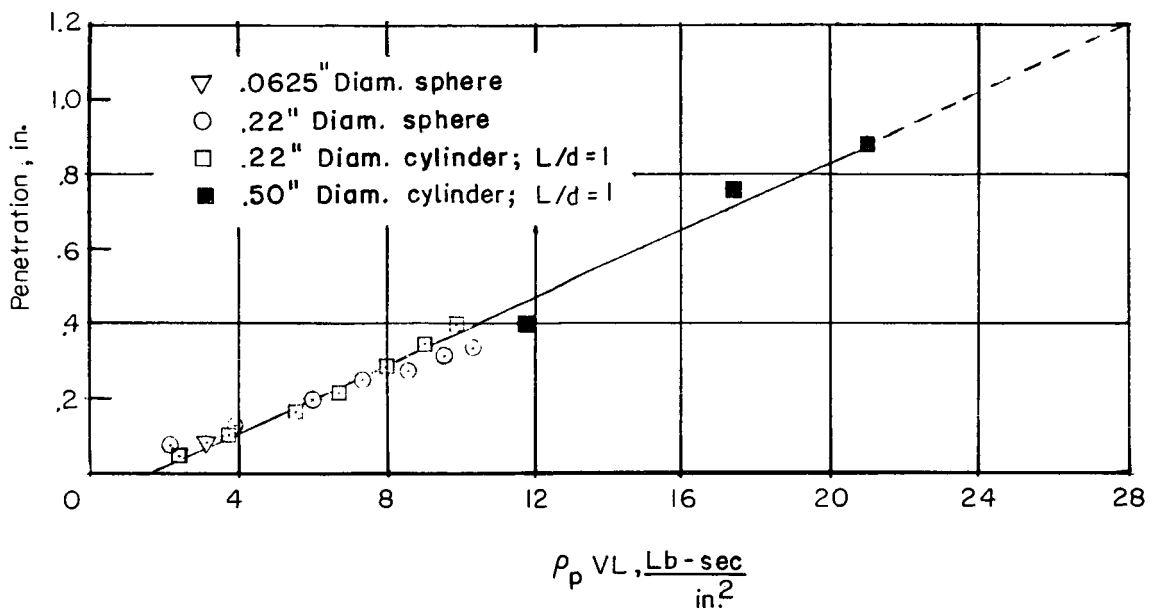

(b) Steel projectile.

Figure 7.- Penetration in aluminum target plotted against momentum per unit area of impacting projectile.

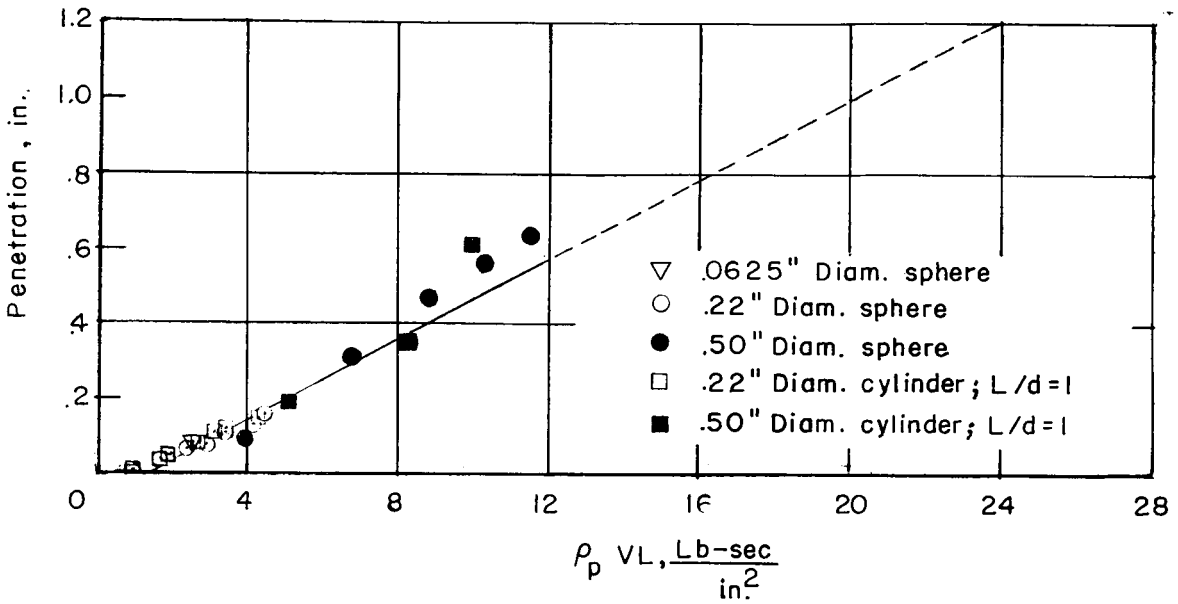

(c) Aluminum projectile.

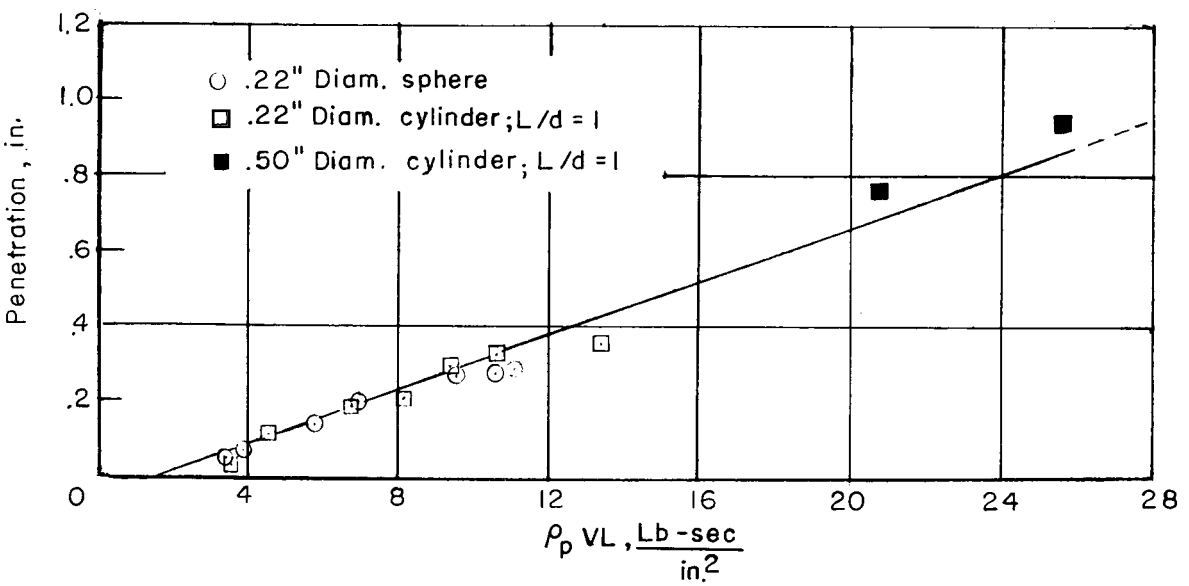

(d) Lead projectile.

Figure 7.- Concluded.

L-766

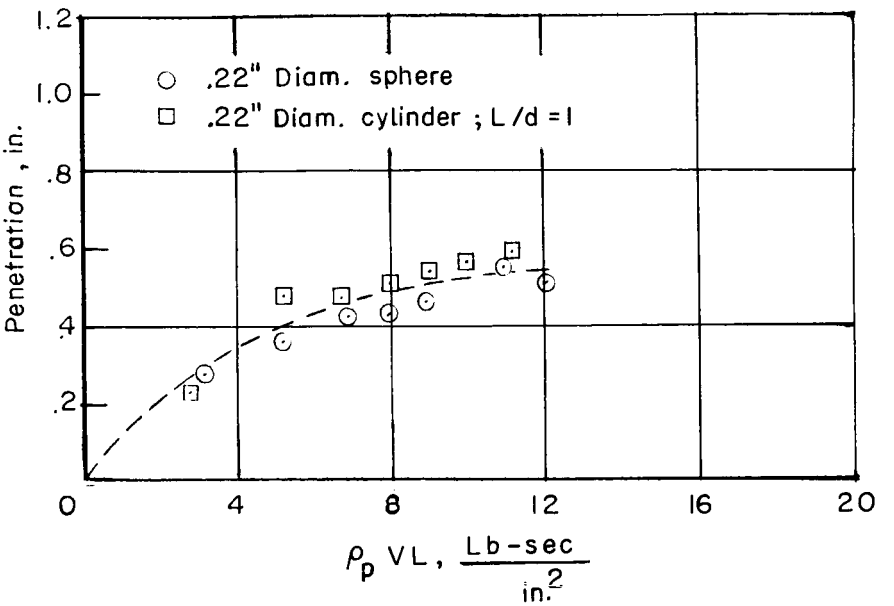

(a) Copper projectile.

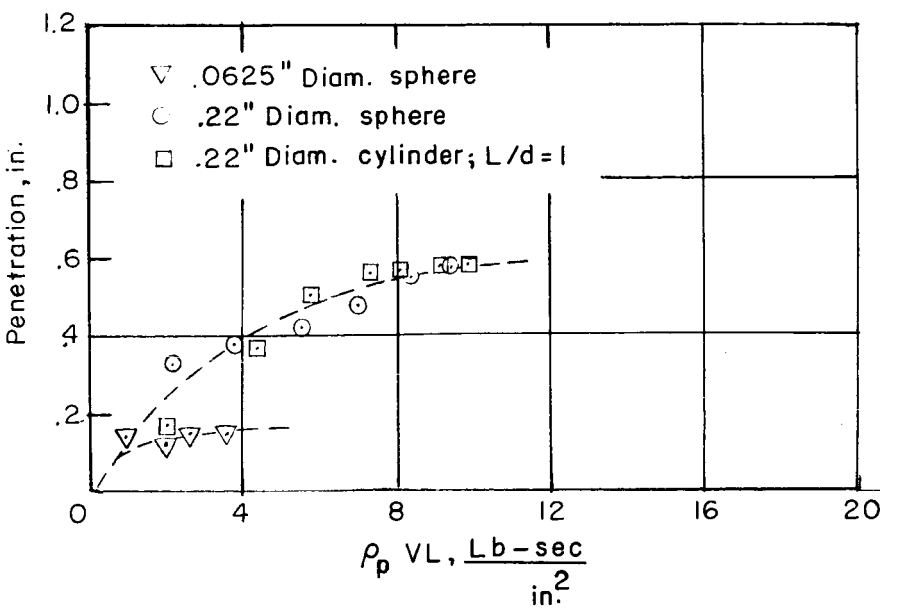

(b) Steel projectile.

Figure 8.- Penetration in lead target plotted against momentum per unit area of impacting projectile.

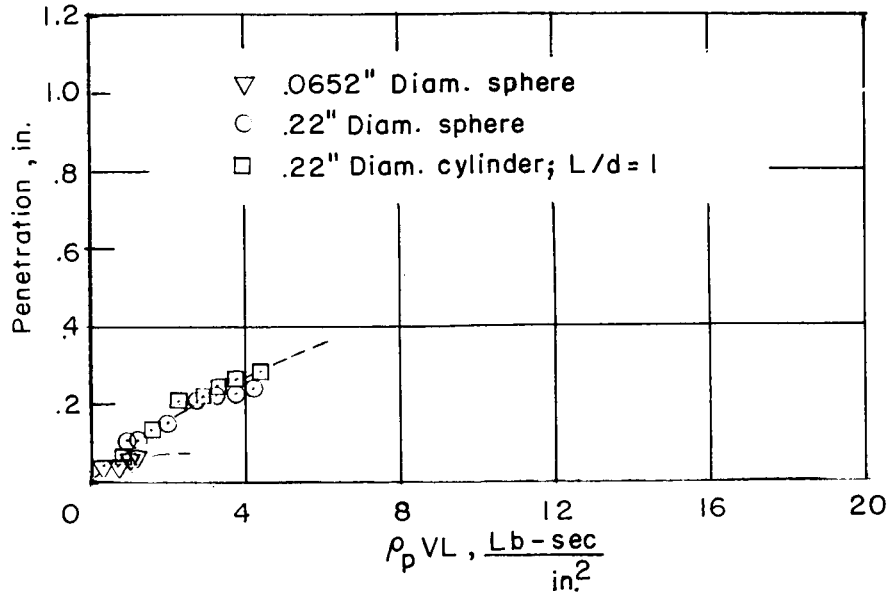

(c) Aluminum projectile.

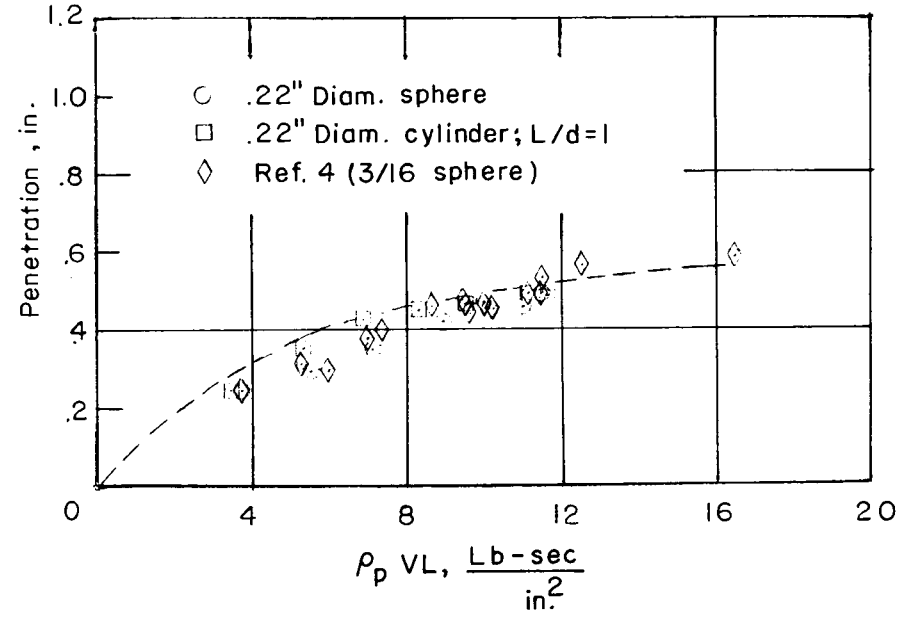

(d) Lead projectile.

Figure 8.- Concluded.

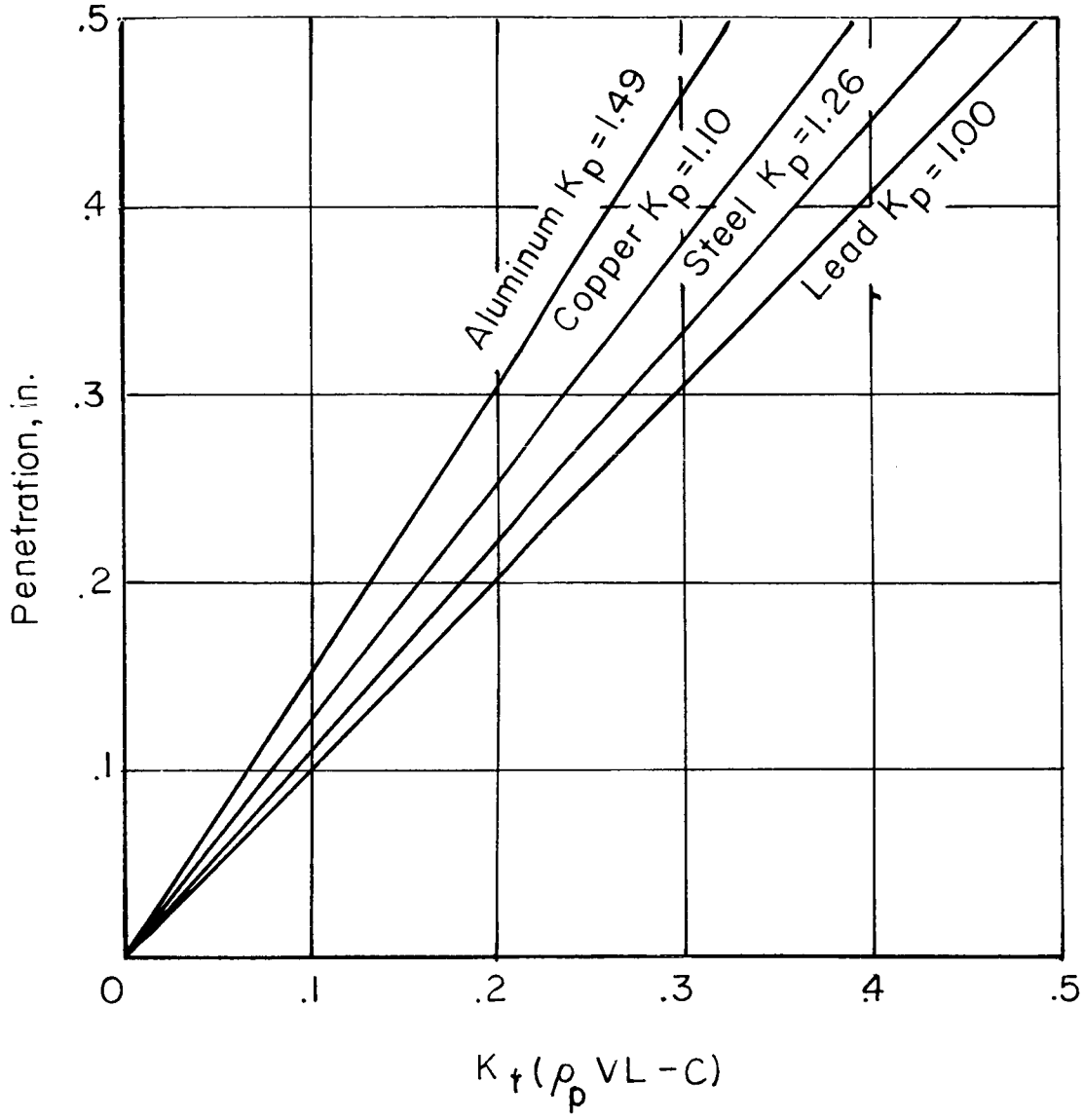

Figure 9.- Effect of projectile deformation factor on magnitude of penetration.

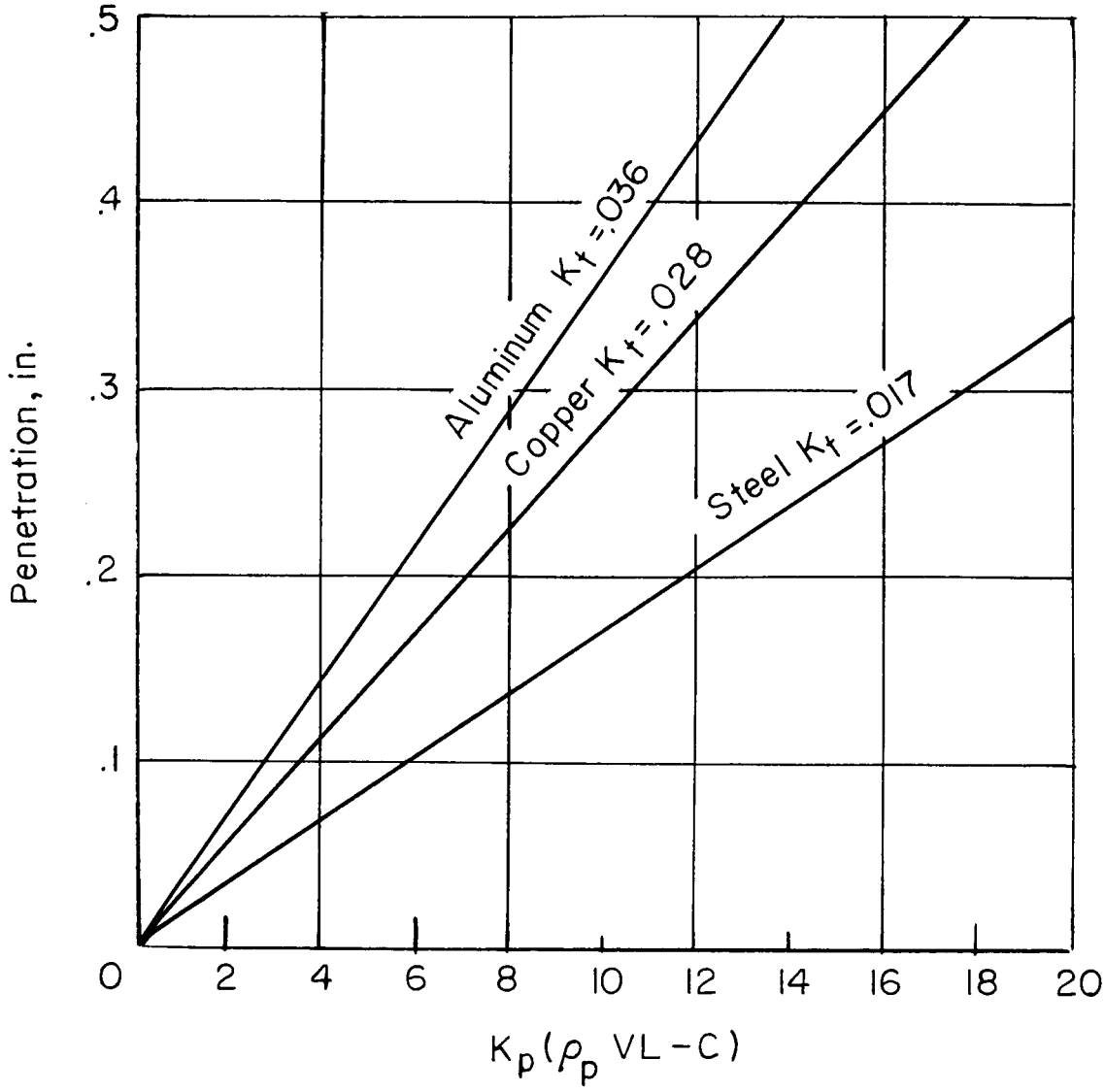

Figure 10.- Effect of target resistance factor on magnitude of penetration.

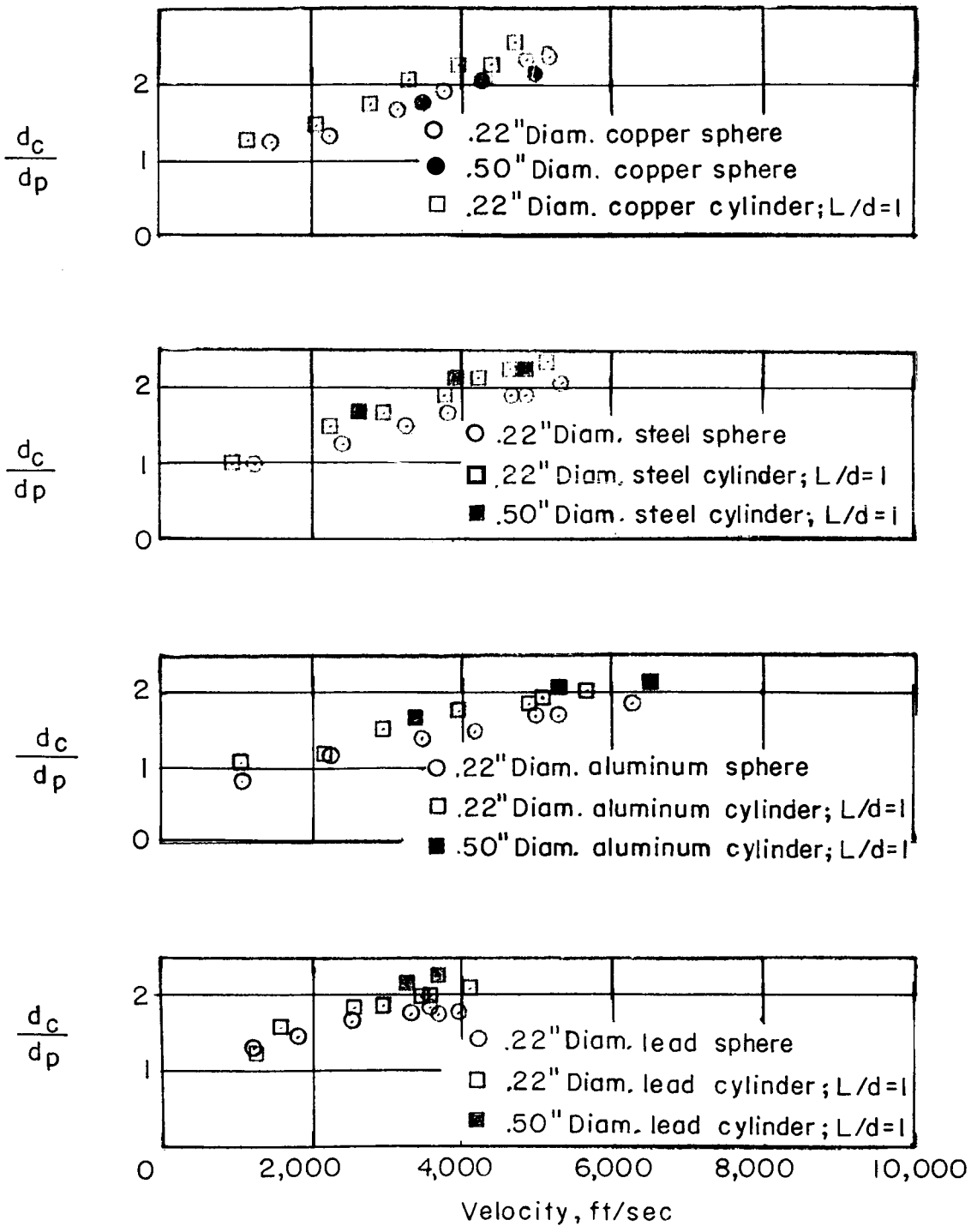

Figure 11.- Crater diameter divided by projectile diameter plotted against velocity for copper targets.

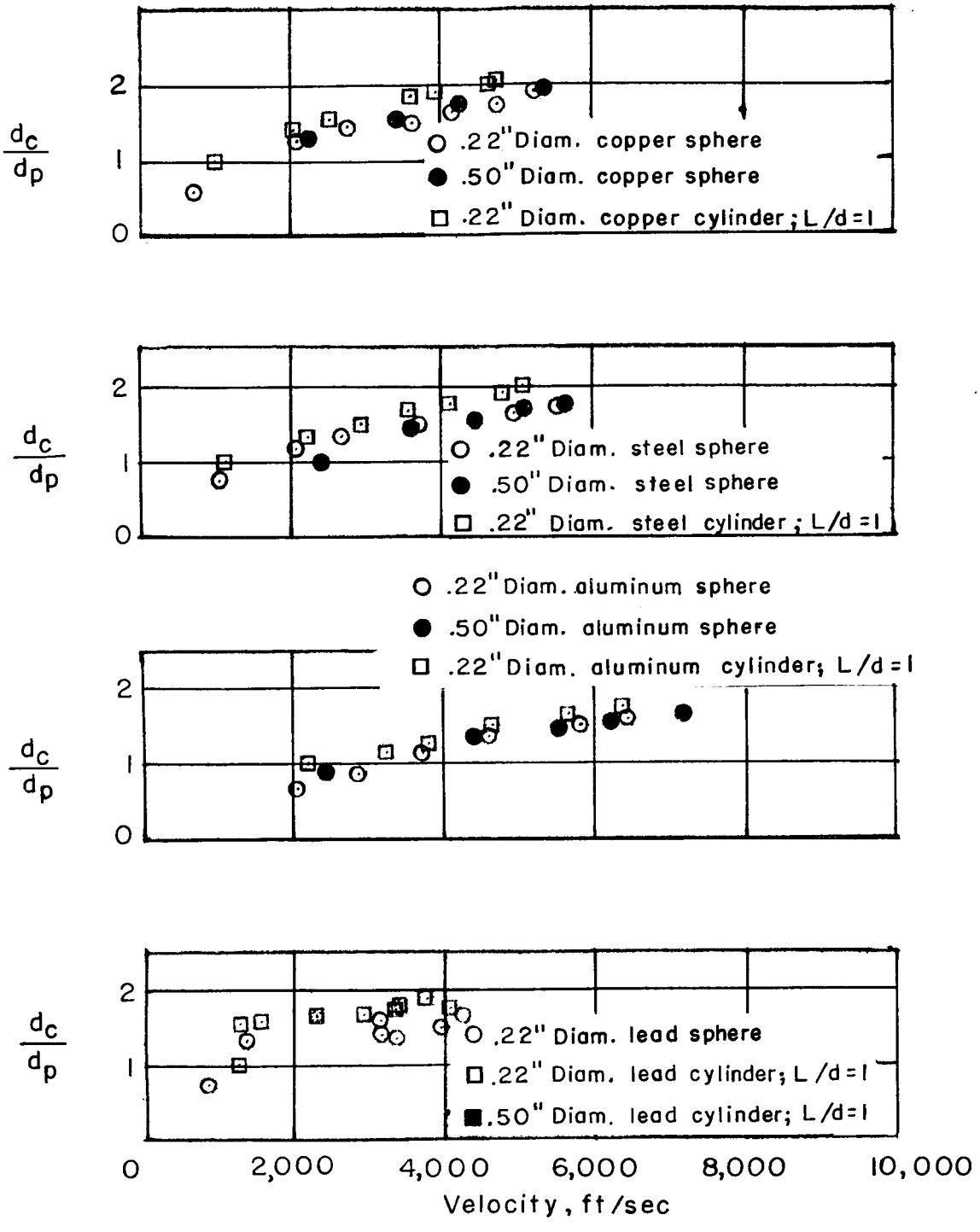

Figure 12.- Crater diameter divided by projectile diameter plotted against velocity for steel targets.

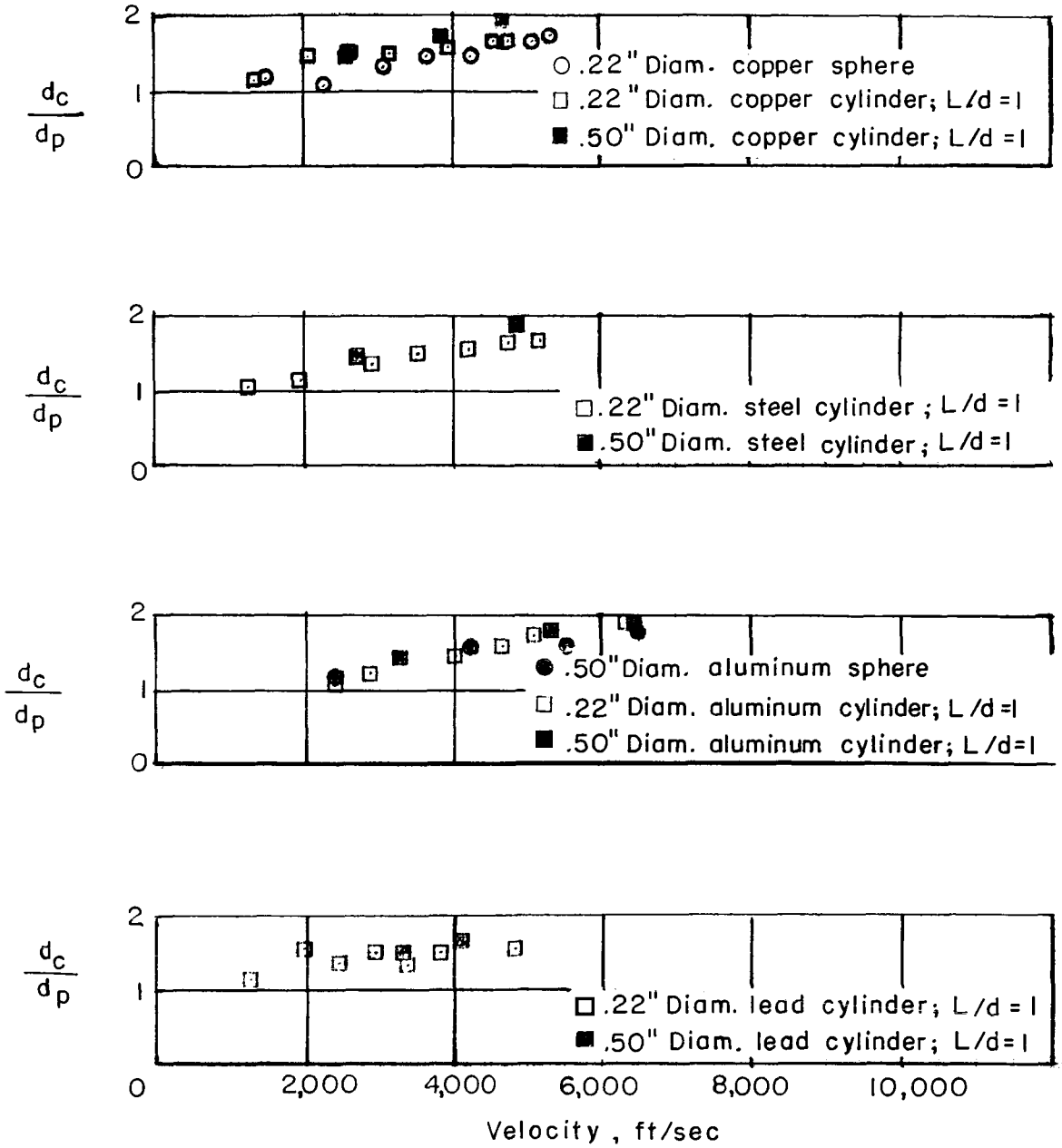

Figure 13.- Crater diameter divided by projectile diameter plotted against velocity for aluminum targets.

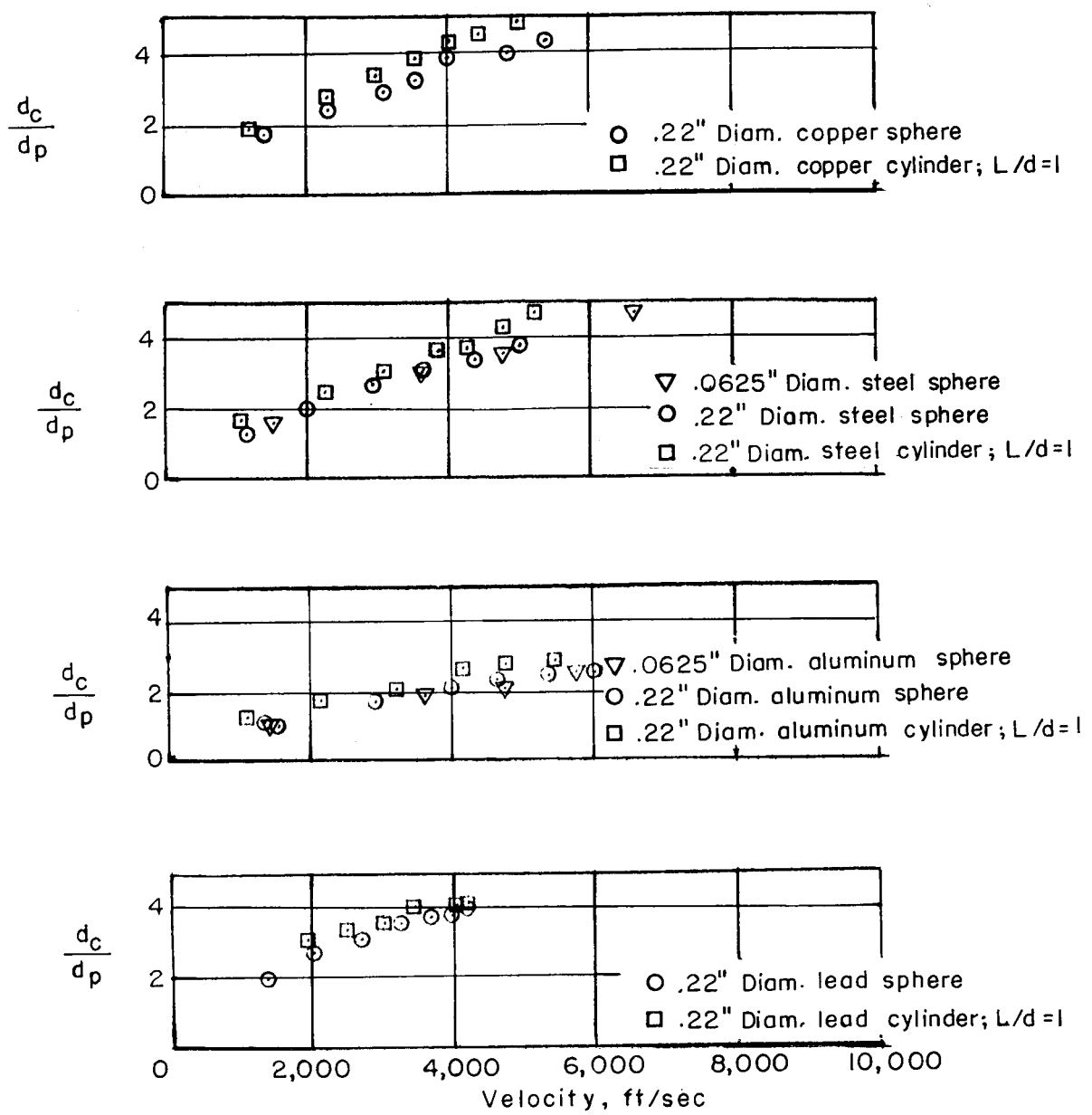

Figure 14.- Crater diameter divided by projectile diameter plotted against velocity for lead targets.

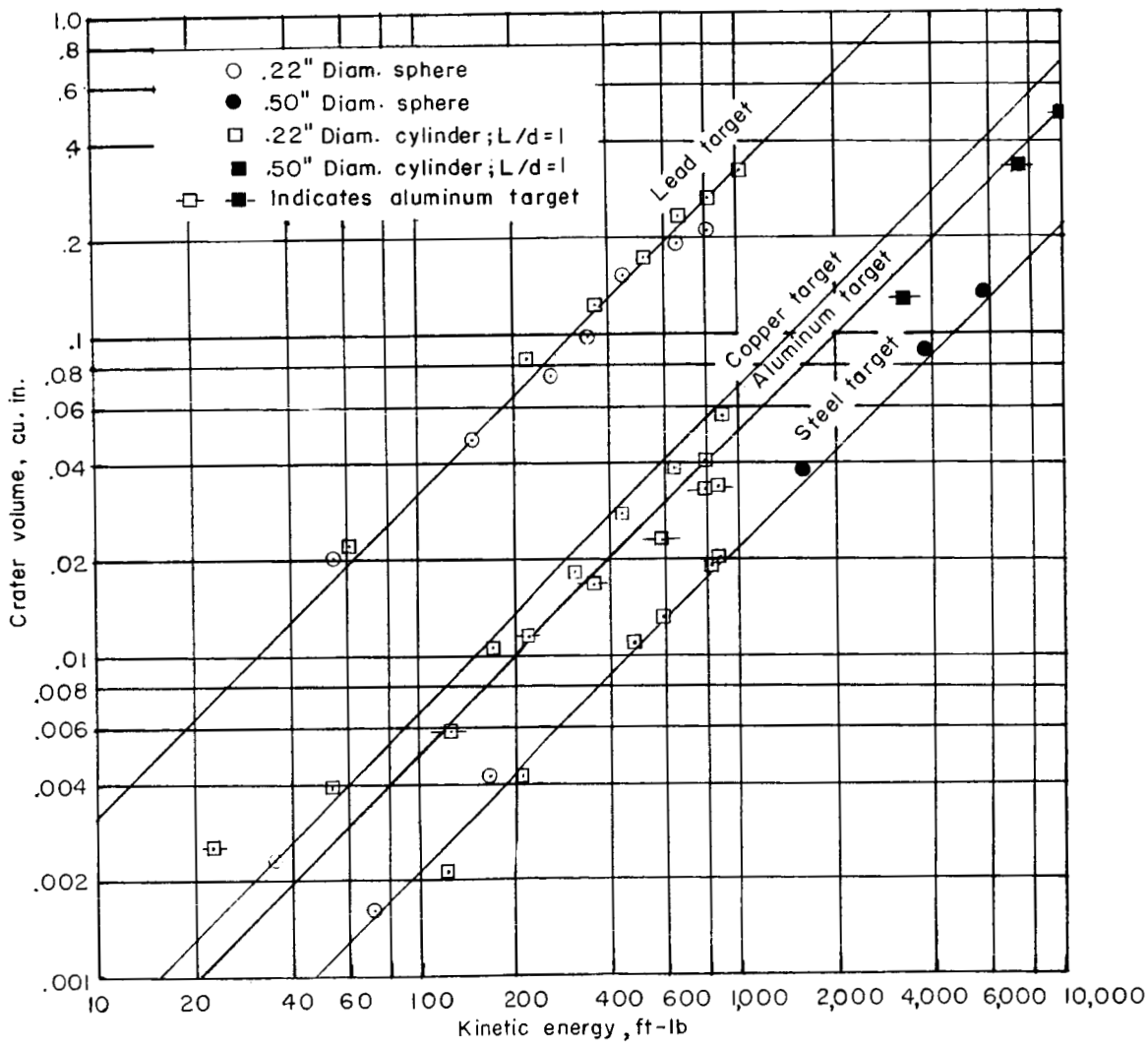

Figure 15.- Crater volume plotted against effective kinetic energy for copper projectiles.

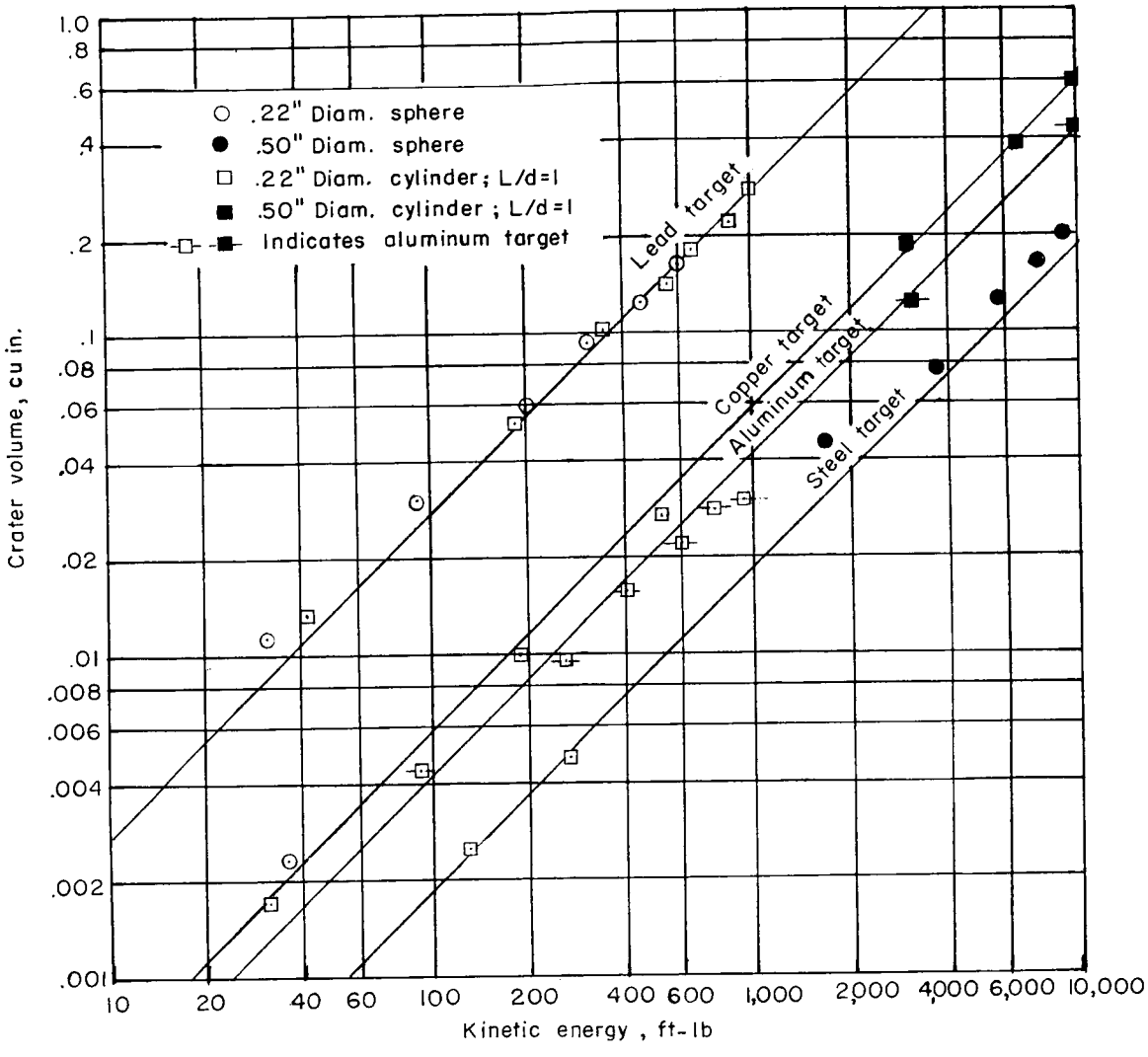

Figure 16.- Crater volume plotted against effective kinetic energy for steel projectiles.

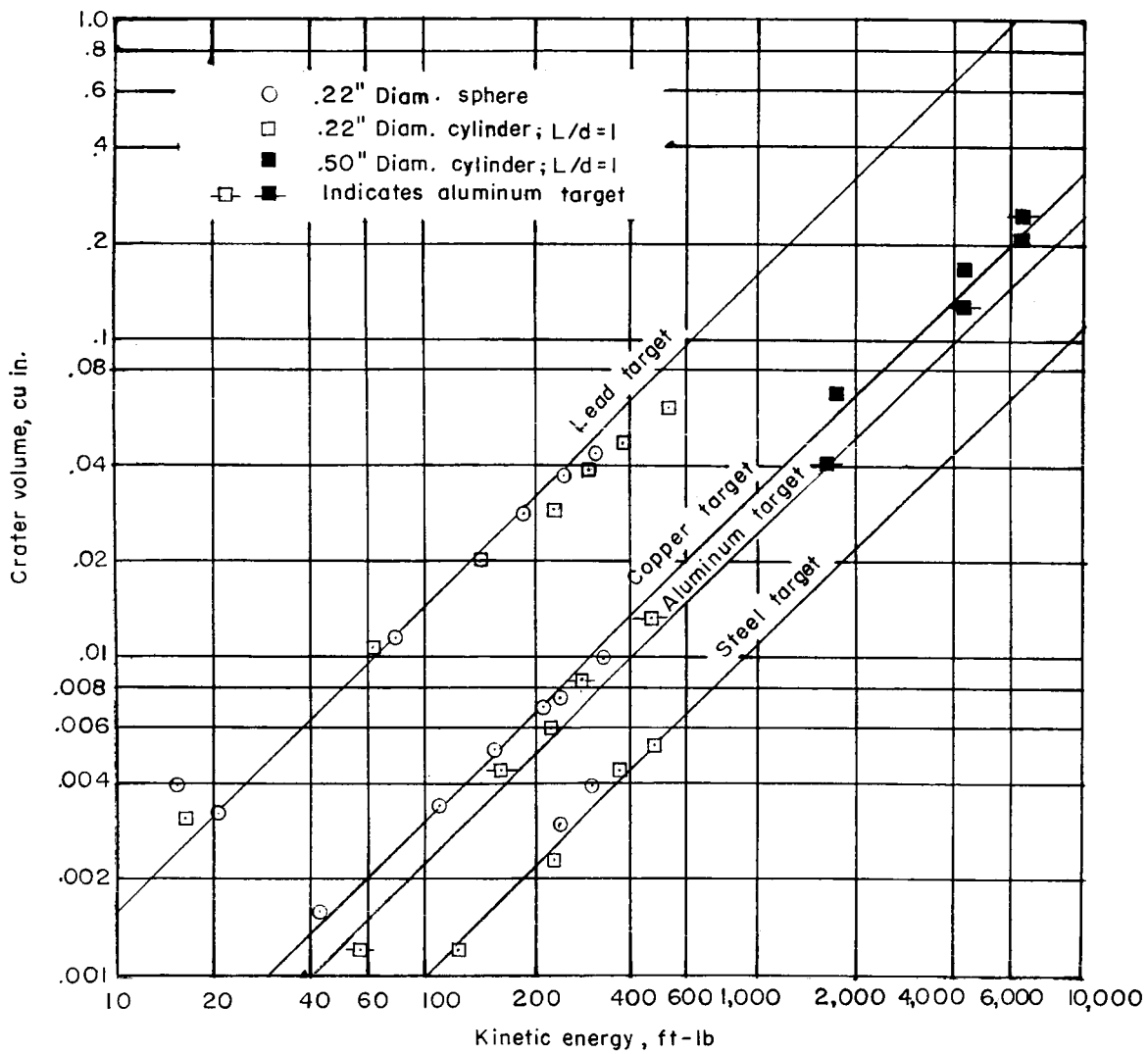

Figure 17.- Crater volume plotted against effective kinetic energy for aluminum projectiles.

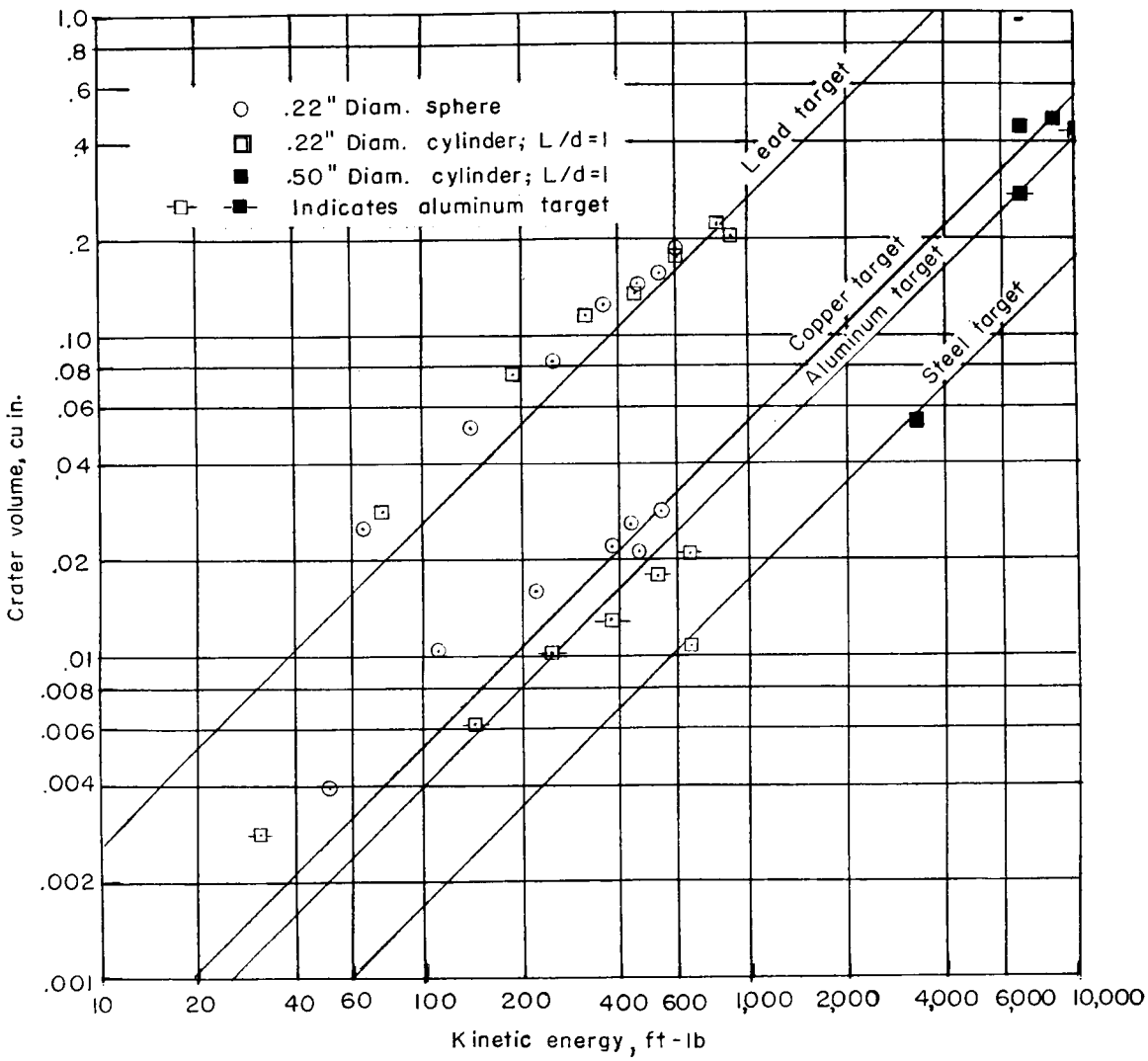

Figure 18.- Crater volume plotted against effective kinetic energy for lead projectiles.

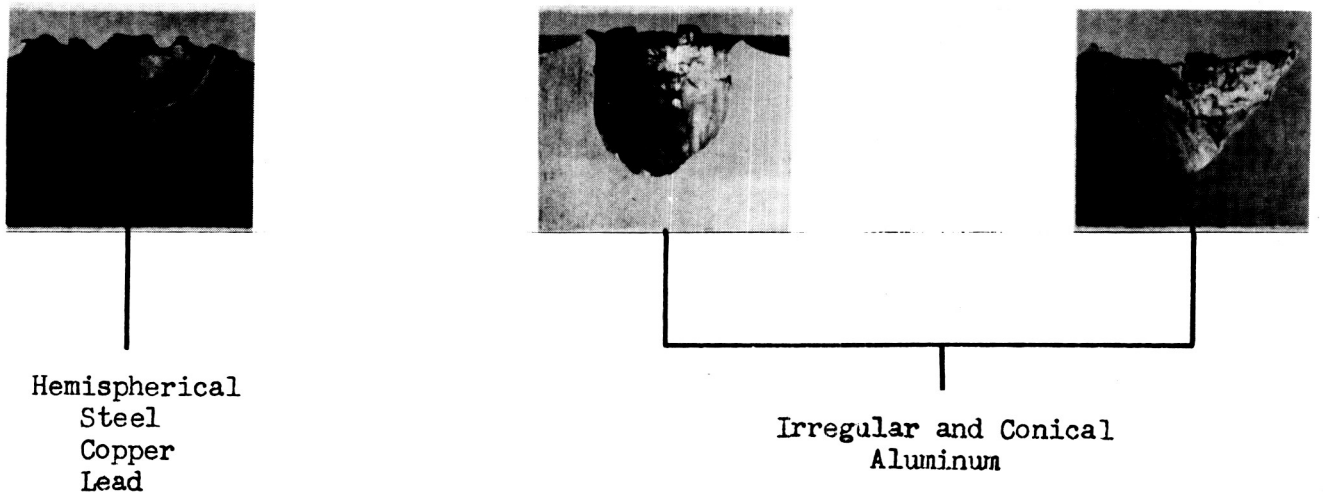

L-59-8213

Figure 19.- Typical crater configurations resulting from high-velocity impacts into aluminum, copper, steel, and lead targets.